Molecular Microbiology (2014) 93(5), 992–1009
doi:10.1111/mmi.12712
First published online 31 July 2014

Distinct characteristics of OxyR2, a new OxyR-type regulator, ensuring expression of Peroxiredoxin 2 detoxifying low levels of hydrogen peroxide in *Vibrio vulnificus*

Suyeon Kim,[1†] Ye-Ji Bang,[1†] Dukyun Kim,[1] Jong Gyu Lim,[1] Man Hwan Oh[2] and Sang Ho Choi[1*]
[1]*National Research Laboratory of Molecular Microbiology and Toxicology, Department of Agricultural Biotechnology, Center for Food Safety and Toxicology, Seoul National University, Seoul 151-921, Korea.*
[2]*Department of Nanobiomedical Science, Dankook University, Cheonan 330-714, Korea.*

Summary

Two peroxiredoxins, Prx1 and Prx2, were previously identified in *Vibrio vulnificus*. Besides OxyR1, a homologue of *Escherichia coli* OxyR (*Ec*OxyR), OxyR2 that shares low homology with *Ec*OxyR was first identified in *V. vulnificus*. OxyR2 activated *prx*2 during aerobic growth, while OxyR1 activated *prx*1 only when exposed to exogenous H_2O_2. OxyR2 was oxidized to form a reversible C206 to C215 disulphide bond by sensing low levels of H_2O_2, which were insufficient to oxidize OxyR1, and only the oxidized OxyR2 activated *prx*2. OxyR2$_{5CA}$, in which all cysteine residues except for C206 and C215 were replaced with alanines, and its mutants, OxyR2$_{5CA}$-C206S and OxyR2$_{5CA}$-C215S, were constructed. OxyR2$_{5CA}$ and OxyR2$_{5CA}$-C215S directly bound to a specific binding sequence centred at –56.5 from the *prx*2 transcription start site, albeit with different binding affinities. The binding sequence consisted of four ATCGnt elements spaced by a helical turn and aligned in the twofold dyad symmetry, suggesting that OxyR2 binds DNA as a tetramer. OxyR2$_{5CA}$-C206S also directly bound to DNA comprising more extended sequences, indicating that oxidized and reduced OxyR2 adopt different conformational states, leading to altered DNA contacts. The *oxyR*2 mutation reduced cytotoxicity and growth during infection, indicating that OxyR2 is essential for the pathogenesis of *V. vulnificus*.

Accepted 8 July, 2014. *For correspondence. E-mail choish@snu.ac.kr; Tel. (+82) 2 880 4857; Fax (+82) 2 873 5095. †Both authors contributed equally to this work.

Introduction

Bacteria continually encounter toxic reactive oxygen species (ROS) that are endogenously produced by incomplete reduction of oxygen during normal aerobic growth and are occasionally increased by exposure to redox-active chemicals in their growth environments (Storz and Zheng, 2000). Oxidative stress caused by increased levels of the ROS such as hydrogen peroxide (H_2O_2) can lead to the damage of all cellular components including DNA, protein and membrane lipid. Particularly, pathogenic bacteria have to cope with oxidative stress imposed by immune systems to survive host environments and in turn to ensure developing illness. Therefore, the bacteria's mechanisms to survive oxidative stress are closely linked to their virulence (Miller and Britigan, 1997). The mechanisms of bacterial defence against oxidative stress include highly specific and effective antioxidant enzymes (Storz and Zheng, 2000). Among the antioxidant enzymes, peroxiredoxins (Prxs) are a family of cysteine-based peroxidases expressed in a wide range of eubacteria (Hall *et al*., 2009). Typical 2-cysteine Prxs have two conserved catalytic cysteines and are the largest group of Prxs. The cysteines are oxidized to reduce peroxides by forming an intermolecular disulphide bond, and the disulphide-bonded Prxs are subsequently reduced and reactivated by thiol-containing reductants such as alkyl hydroperoxidase subunit F (AhpF) and thioredoxin (TrxA) (Hall *et al*., 2009).

AhpC (alkyl hydroperoxidase subunit C), one of the best characterized 2-cysteine Prxs and utilizing AhpF as a reductant to compose an NAD(P)H-dependent peroxidase system, was originally identified from *Escherichia coli* and *Salmonella typhimurium* (Christman *et al*., 1985; Jacobson *et al*., 1989; Storz *et al*., 1989). Expression of AhpC is activated by OxyR, which is a central regulator of the oxidative stress response in a number of bacteria (for a recent review see Dubbs and Mongkolsuk, 2012). Typical OxyR, such as *E. coli* OxyR (*Ec*OxyR) is a modular structure consisting of an N-terminal DNA binding domain (DBD) and C-terminal regulatory and multimerization domain that contains two conserved redox-sensitive cysteines, sensing (C199) and resolving (C208)

cysteines (Kullik *et al*., 1995a,b; Zheng *et al*., 1998). OxyR senses peroxides via direct oxidation of the sensing cysteine residue. Although only the oxidized OxyR is the active form that can activate transcription *in vitro* and *in vivo*, the exact mechanism of oxidant sensing that activates OxyR is still controversial (Dubbs and Mongkolsuk, 2012). One possible mechanism is a molecular code hypothesis and suggests that modification of the C199 alone is sufficient to activate OxyR without formation of a disulphide bond and the type of modification results in the distinct regulatory outcome (Kim *et al*., 2002; Seth *et al*., 2012). The other one is that the C199 is oxidized by H_2O_2 to a cysteine sulphenic acid intermediate (C199-SOH), which is followed by the formation of an intramolecular disulphide bond with C208 (Zheng *et al*., 1998; Åslund *et al*., 1999; Lee *et al*., 2004). This oxidation induces large conformational changes in the regulatory domain leading to altered associations between the subunits within the tetramer and altered DNA binding pattern, and in turn allowing productive interaction between OxyR and RNA polymerase (RNAP) (Toledano *et al*., 1994; Choi *et al*., 2001; Lee *et al*., 2004).

In a facultative aerobic pathogen *Vibrio vulnificus*, two distinct Prxs, Prx1 and Prx2, have been identified (Baek *et al*., 2009; Bang *et al*., 2012). Prx1 (formerly *V. vulnificus* AhpC) is highly homologous to other bacterial Prxs such as *E. coli* AhpC (78% identity in amino acid sequences) and is an AhpF dependent peroxidase (Baek *et al*., 2009). Prx1 is expressed only in cells exposed to high levels of H_2O_2 and effective at decomposing large amounts of peroxides rapidly as evidenced by its high turnover rate and efficient reactivation by AhpF (Bang *et al*., 2012). The *ahpF* gene is located immediately downstream of *prx*1 and the *prx*1 and *ahpF* genes are organized in the same orientation as in *E. coli ahpC* and *ahpF* (Baek *et al*., 2009). In contrast to Prx1, Prx2 is a novel Prx that shares limited amino acid sequence homology with other bacterial Prxs and AhpC. Prx2 is a TrxA dependent peroxidase and more effective for the reduction of low levels of H_2O_2 because of its high affinity to H_2O_2. Prx2 expression is induced by trace amounts of H_2O_2, which suggests that Prx2 is a scavenger of H_2O_2 generated endogenously by aerobic metabolism. Therefore, having two Prxs in which the expression patterns and kinetic properties are differentially optimized for the most efficient decomposition of distinct levels of H_2O_2 could provide an evolutionary advantage for the survival of *V. vulnificus* encountering various ranges of oxidative stress. In this context, the division of duty in detoxifying oxidative stress has been observed previously in a wide range of bacteria. AhpC and catalases scavenge low and high levels of H_2O_2 in *E. coli* respectively (Seaver and Imlay, 2001). Similarly, the *ahp*C mutation leads to compensatory induction of the synthesis of a catalase (KatA) in *Bacillus subtilis* (Bsat *et al*., 1996).

Although the two Prxs have been well characterized kinetically, the molecular mechanisms by which *V. vulnificus* modulates the discrete expression of Prx1 and Prx2 in response to different levels of H_2O_2 have not been yet addressed. The similarity found in deduced amino acid sequences and genetic organization between *prx*1 and *E. coli ahpC* indicates that *prx*1 expression could be also regulated by OxyR (or a homologue). *V. vulnificus* OxyR (hereafter OxyR1) was found previously (Kong *et al*., 2004), and the alignment of the deduced amino acid sequences of OxyR1 to those of *Ec*OxyR reveals a high level (63%) of identity (http://blast.ncbi.nlm.nih.gov/Blast.cgi). However, OxyR1 regulation of the *prx*1 expression has not yet been experimentally verified. Furthermore, neither the promoter(s) of *prx*2 nor any *trans*-acting regulatory protein(s) required for the expression of *prx*2 has been previously identified. In the present study, we identified a novel OxyR-type transcriptional regulator of *V. vulnificus*, OxyR2, which is required for the expression of Prx2. Characterization of OxyR2 in comparison with OxyR1 provided evidence that OxyR2 is activated by forming a reversible disulphide bond in response to low levels of H_2O_2 that are insufficient to activate OxyR1. Also, binding of OxyR2 directly to the upstream region of *prx*2 was demonstrated, and the sequence for OxyR2 binding was determined. Finally, the possible role of OxyR2 in *V. vulnificus* pathogenesis was investigated.

Results

Identification and sequence analysis of V. vulnificus *OxyR2*

In the course of sequence analysis of the *V. vulnificus* MO6-24/O genome (GenBank™ CP002469 and CP002470), a coding region was identified immediately upstream of *prx*2 (Fig. 1A). The coding region was transcribed divergently from *prx*2, and its deduced amino acid sequences revealed a putative LysR-type transcriptional regulator composed of 301 amino acids with a theoretical molecular mass of 33,543 Da and a pI of 5.58 (Fig. 1A and B). A database search for homology to the amino acid sequence of the putative regulator singled out OxyR1 and *Ec*OxyR. Although the putative regulator was only 34% and 37% identical in amino acid sequences to those of OxyR1 and *Ec*OxyR, respectively, the protein has the putative redox-sensitive cysteine residues, C206 and C215, which roughly correspond to C199 and C208 respectively, in *Ec*OxyR (Zheng *et al*., 1998; Lee *et al*., 2004) (Fig. 1B). OxyR2 contains a helix–turn–helix motif in the N-terminal DNA binding domain (DBD) and the residues of *Ec*OxyR that have been implicated in the activation of RNAP (Kullik *et al*., 1995a; Choi *et al*., 2001;

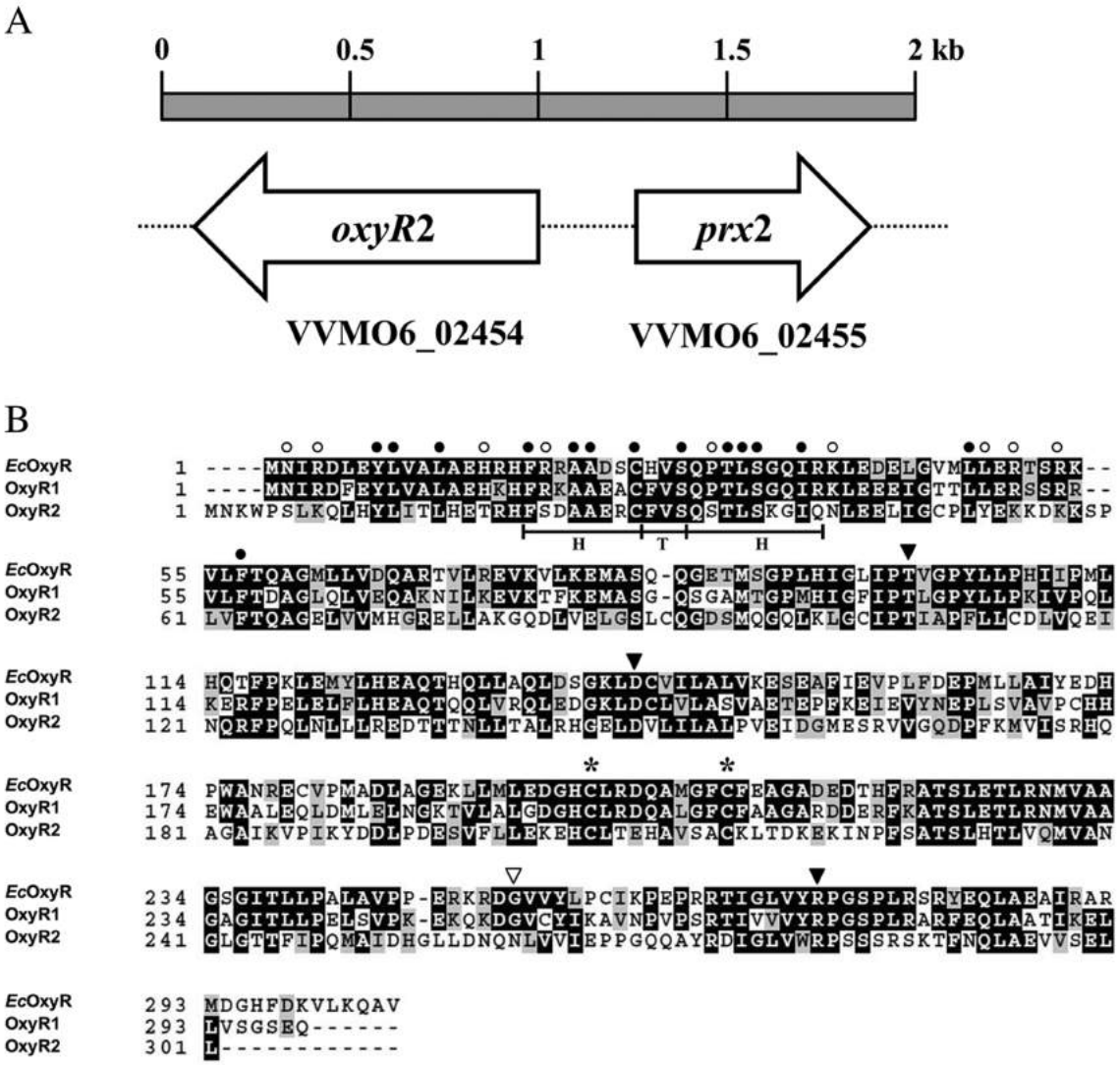

Fig. 1. Physical map of *V. vulnificus oxyR*2 and *prx*2, and amino acid sequence relatedness of bacterial OxyRs.
A. The arrows represent the coding regions of *oxyR*2 (VVMO6_02454) and *prx*2 (VVMO6_02455). The figure was derived using the nucleotide sequences of the *V. vulnificus* MO6-24/O genome (GenBank™ CP002469 and CP002470).
B. The amino acid sequences retrieved from NCBI protein database (NCBI, http://www.ncbi.nlm.nih.gov) (accession numbers NP_418396 for *Ec*OxyR, ADV85339 for OxyR1, ADV87476 for OxyR2) were aligned using the CLUSTALW program (http://www.ch.embnet.org/software/ClustalW.html). Identical sequences (*black boxes*), similar sequences (*gray boxes*), two conserved redox-sensitive cysteines (*asterisks*), missing sequences (*dashes*), and the region of HTH motif (*bars*) are indicated. The residues of *Ec*OxyR that are previously predicted to be important for DNA binding (*circles*) and RNAP activation (*triangles*) are indicated above the amino acid sequence. Among them, the residues conserved in OxyR2 are indicated by filled symbols whereas those not conserved in OxyR2 are indicated by open symbols. *Ec*OxyR, *E. coli* OxyR; OxyR1, *V. vulnificus* OxyR1; OxyR2, *V. vulnificus* OxyR2.

Zaim and Kierzek, 2003; Wang *et al*., 2006) (Fig. 1B). The combined information suggested that the putative regulator is an OxyR-type transcriptional regulator, and thereby was named *V. vulnificus* OxyR2. However, many residues of *Ec*OxyR DBD that are predicted to play an important role or to directly participate in DNA binding are not conserved in OxyR2 DBD (Fig. 1B). This difference in DBD indicated that the DNA sequences for binding of OxyR2 could be different from those of *Ec*OxyR.

OxyR2 is distinct from OxyR1 in regulation of peroxiredoxins

We previously demonstrated the coexistence of the two peroxiredoxins, Prx1 and Prx2 along with their distinct roles in a single bacterium, *V. vulnificus* (Baek *et al*., 2009; Bang *et al*., 2012). Expression levels of *prx*2 and *prx*1 in the strains grown aerobically were compared by Northern blot analyses (Fig. 2). When total RNA was isolated from

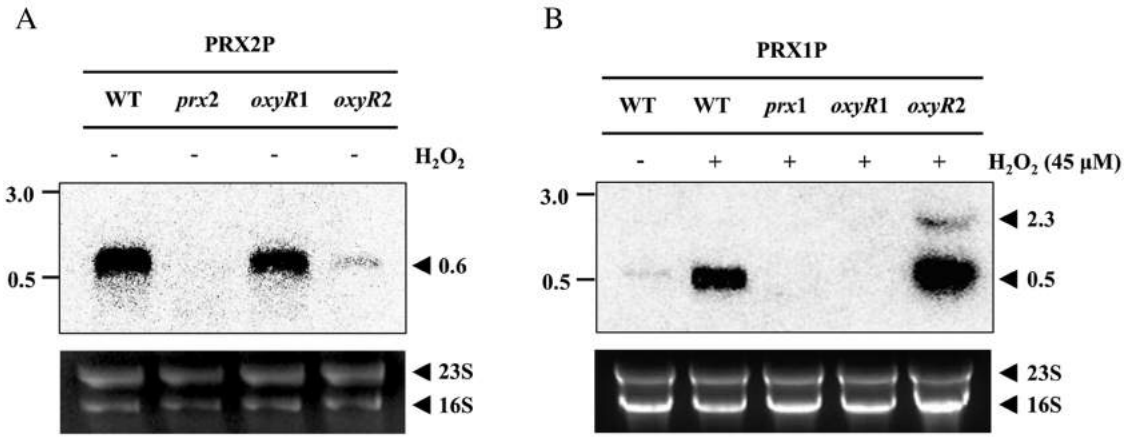

Fig. 2. Effect of *oxyR*2 and *oxyR*1 mutation on the expression of *prx*2 and *prx*1. The levels of the *prx*2 (A) and *prx*1 (B) transcripts in the wild type and mutants which lack OxyR1 or OxyR2 were compared by Northern blot analyses. Total RNAs were isolated from the cultures grown aerobically to an A_{600} of 0.5 and exposed to different concentrations of H_2O_2 for 30 s as indicated. The RNAs were resolved and hybridized to [α-^{32}P]-labelled DNA probe corresponding to the internal coding regions of *prx*2 (PRX2P, A) or *prx*1 (PRX1P, B). The RNA size markers (0.5–10 kb RNA Ladder; Invitrogen) and the *prx* transcripts are shown in kilobases. WT, wild type; *prx*2, *prx*2 mutant; *oxyR*1, *oxyR*1 mutant; *oxyR*2, *oxyR*2 mutant; *prx*1, *prx*1 mutant.

the wild type cells unexposed to exogenous H_2O_2 and hybridized with the PRX2P as a DNA probe, expression of *prx*2 was fully induced (Fig. 2A). This expression of *prx*2 and its independence on exogenous H_2O_2 can be explained from our previous report that Prx2 is a peroxidase that is induced by low levels of endogenous H_2O_2 in the cells of aerobic media (Bang *et al*., 2012). The results in Fig. 2A exhibit that the *prx*2 transcript level of the *oxyR*2 mutant was significantly lower than that of the wild type. In contrast, the *prx*2 transcript level did not significantly differ between the RNA of the *oxyR*1 mutant and the wild type, indicating that OxyR2, but not OxyR1, positively regulates the expression of *prx*2 (Fig. 2A). Interestingly, the *prx*2 transcript is still detectable in the RNA of the *oxyR*2 mutant, indicating that part of the *prx*2 expression is either constitutive or independent on the OxyR2 activity in the cells during aerobic growth.

When PRX1P was used as a DNA probe, Northern blot analyses demonstrated that the 0.5 kb *prx*1 transcript was not apparent unless the aerobically grown cells were exposed to 45 μM H_2O_2. The result is consistent with our previous observation that Prx1 is conditionally expressed upon exposure to high levels of H_2O_2 (Bang *et al*., 2012). The level of the *prx*1 transcript decreased in the *oxyR*1 mutant but not *oxyR*2 mutant, indicating that expression of *prx*1 is positively regulated by OxyR1 (Fig. 2B). It is noteworthy that the level of the *prx*1 transcript in the *oxyR*2 mutant was higher than that of the wild type (Fig. 2B). When determined using the cells grown aerobically without exposure to exogenous H_2O_2, *prx*1 expression of the *oxyR*2 mutant was also higher than that of the parental wild type (Fig. S1). These results are consistent with our previous observation that Prx2 is a residential scavenger of peroxides generated endogenously and thus the lack of Prx2 (due to the lack of OxyR2) accumulated sufficient H_2O_2 to induce the expression of Prx1 (Bang *et al*., 2012). Interestingly, PRX1P also hybridized to approximately 2.3 kb RNA when the RNA was isolated from the *oxyR*2 mutant (Fig. 2B). On the basis of the DNA sequence of *prx*1*ahpF*, it was anticipated that a polycistronic *prx*1*ahpF* transcript would be approximately 2.3 kb long (Baek *et al*., 2009). Northern blot analysis was performed using the *ahpF* coding region as a DNA probe, and a single mRNA corresponding to the *prx*1*ahpF* transcript was detected, confirming that the *prx*1*ahpF* genes were partially transcribed as a single operon as suggested by Fig. 2B (data not shown). Therefore, it appeared that the *prx*1*ahpF* genes, at least in part, are co-transcribed to result in the *prx*1*ahpF* transcript (Fig. 2B).

OxyR2 is oxidized by H_2O_2 *to form a reversible C206 to C215 disulphide bond*

When the *oxyR*2 mutant cells containing pDY1025 expressing wild-type OxyR2 were grown either anaerobically or aerobically and alkylated with 4-acetamido-4′-maleimidylstilbene-2, 2′-disulphonic acid (AMS) (Invitrogen, Carlsbad, CA), the molecular size of the resulting alkylated OxyR2 decreased by approximately 1 kDa in the aerobically grown cells (Fig. 3A). Since the molecular weight of AMS is approximately 0.5 kDa, the 1 kDa decrease may represent the elimination of two free thiols in OxyR2 in the aerobically grown cells. When the anaerobically grown cells were exposed to 10 μM of H_2O_2 for various time intervals and then alkylated with AMS, the 1 kDa decreased OxyR2 appeared at 0.5 min

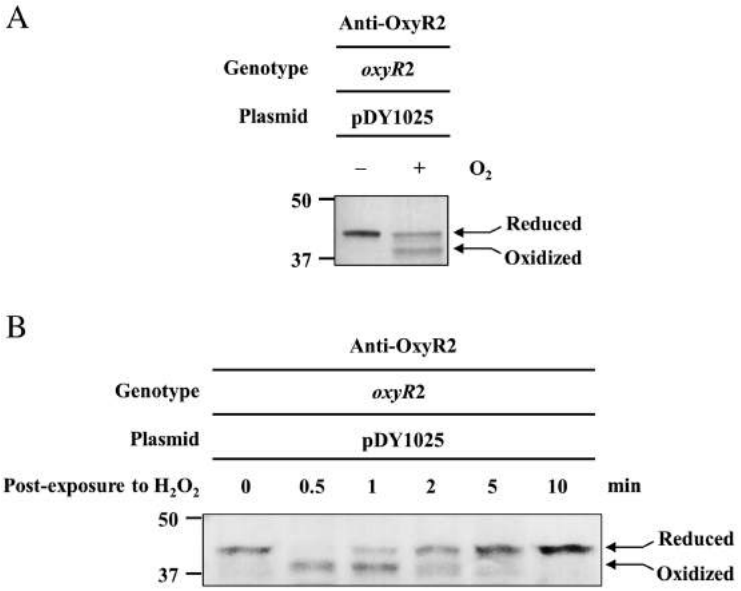

Fig. 3. A reversible disulphide bond formation of OxyR2.
A. The *oxyR*2 mutant containing pDY1025 expressing wild-type OxyR2 was grown anaerobically to an A_{600} of 0.3 or aerobically to an A_{600} of 0.5, and cells were immediately harvested without additional exposure to H_2O_2.
B. The *oxyR*2 mutant containing pDY1025 expressing wild-type OxyR2 was grown anaerobically to an A_{600} of 0.3. Upon exposure to 10 μM H_2O_2, cells were harvested at various time intervals as indicated. (A and B) Cells were then precipitated with TCA and alkylated with fresh AMS buffer for 1 h at 37°C. Alkylated OxyR2s were resolved by non-reducing SDS-PAGE and immunoblotted using the rabbit anti-OxyR2 antibody. The protein size markers (Precision Plus Protein Standards; Bio-Rad Laboratories, Hercules, CA) are shown in kilodaltons and the two conformations (reduced and oxidized forms) of OxyR2 (*arrows*) are indicated.

after exposure to H_2O_2 (Fig. 3B). This indicated that sensing of H_2O_2 by OxyR2 occurs by redox-sensitive modification of two specific cysteine residues such as formation of a single intramolecular disulphide bond. The decreased molecular size of the alkylated OxyR2 was recovered by 10 min after H_2O_2 treatment (Fig. 3B), indicating that the modification was reversed when the oxidative stress was relieved.

Similarly, the *oxyR*2 mutant containing plasmids expressing mutant OxyR2, in which each of the seven cysteines was mutated to serine, respectively, were grown anaerobically and then subjected to the AMS alkylation assay to identify redox-sensitive cysteines. When the cells harbouring plasmids expressing OxyRs with C29S, C49S, C91S, C104S and C114S mutations were alkylated with AMS, the 1 kDa decreases in molecular size of the mutant OxyR2 were still observed in the H_2O_2-treated cells. This indicated that the C29, C49, C91, C104 and C114 residues were not involved in modification upon exposure to H_2O_2 (Fig. 4). In contrast, the decrease in molecular size were not detected for both alkylated OxyR2-C206S and -C215S regardless of exposure to H_2O_2, indicating that both mutant OxyRs are unable to undergo the modification when exposed to H_2O_2. These results indicated that the conserved cysteines, C206 and C215 are the redox-sensitive cysteines participating in the redox-sensitive modification of OxyR2 (Fig. 4).

From these results, it seems reasonable to assume that OxyR2 is a redox-sensing regulator and activated by a mechanism similar to that of *Ec*OxyR, in which C206 (as a sensing cysteine) is oxidized by sensing H_2O_2 and forms a disulphide bond with the resolving cysteine C215. Accordingly, the disulphide bond formation between C206 and C215 was examined by MALDI-TOF-MS analysis *in vitro*. Mass spectra for the tryptic digests of each reduced and oxidized OxyR2, in which reduced cysteines were alkylated with iodoacetamide, were compared (Fig. 5). In the reduced OxyR2, peptides containing alkylated C49, C91, C104, C114, C206 and C215 were detected

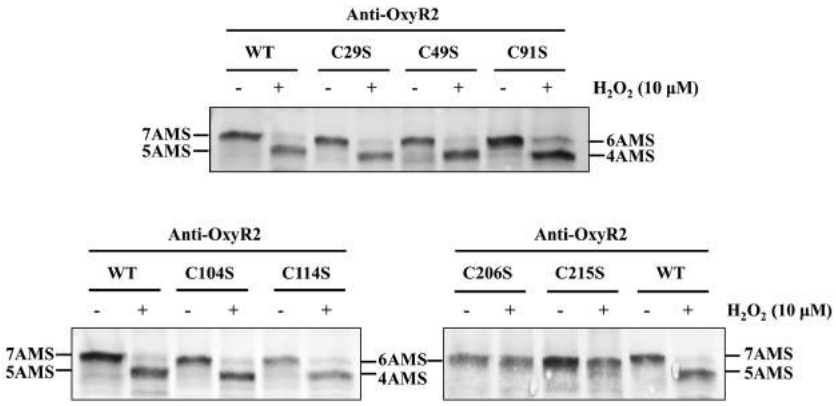

Fig. 4. Identification of the redox-sensitive cysteines of OxyR2. The *oxyR*2 mutant containing plasmids expressing wild-type (WT) or mutant OxyR2s (each of seven cysteines was mutated to serine as indicated) were grown anaerobically to an A_{600} of 0.3. The cultures were treated (+) or not treated (–) with 10 μM H_2O_2 for 30 s, precipitated with TCA, and incubated with fresh AMS buffer for 1 h at 37°C for alkylation of free-thiols in cells. The alkylated OxyR2s were resolved by non-reducing SDS-PAGE and detected by Western blot analysis using the rabbit anti-OxyR2 antibody. The predicted numbers of AMS that alkylated each OxyR2 are shown at the ends of the gel.

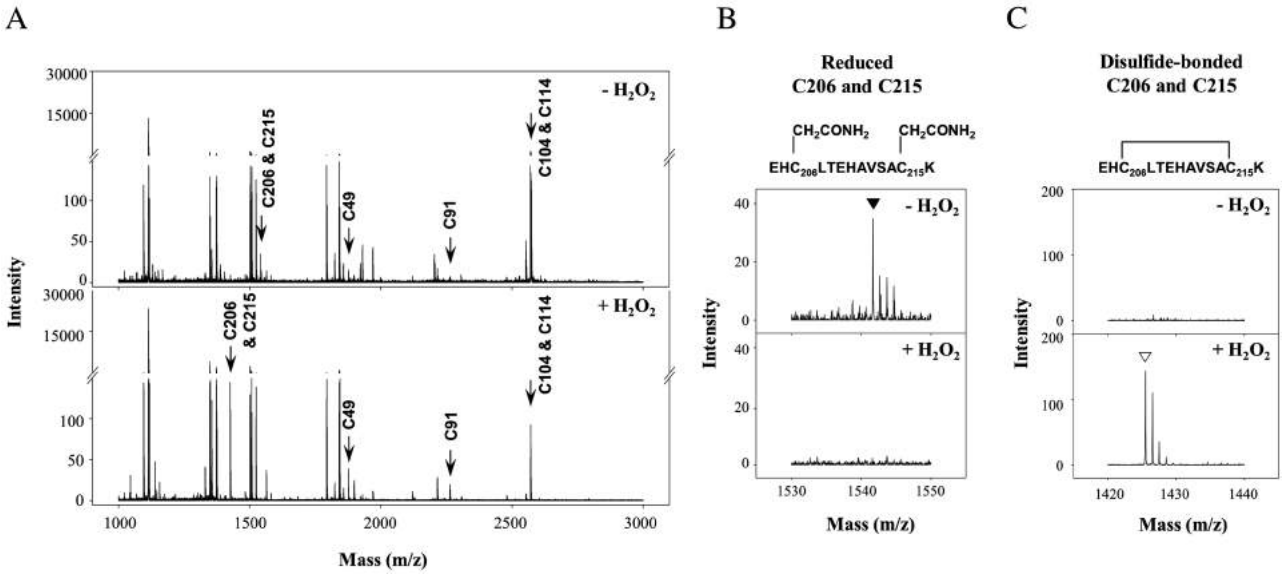

Fig. 5. MALDI-TOF-MS spectra for the tryptic digests of reduced ($-H_2O_2$) and oxidized ($+H_2O_2$) OxyR2. His_6-tagged wild-type OxyR2 protein was reduced with 100 mM DTT for 1 h and desalted by gel filtration chromatography under anaerobic condition. Oxidized OxyR2 was prepared by reacting the reduced OxyR2 with H_2O_2 for 5 min. Each of the reduced and oxidized OxyR2 was then incubated with iodoacetamide to alkylate reduced cysteine residues and digested with trypsin.
A. Mass spectra of reduced ($-H_2O_2$, *upper panel*) and oxidized ($+H_2O_2$, *lower panel*) OxyR2 were presented. Peptides containing cysteines were marked with arrows and labelled according to the residue number of the cysteine.
B and C. Mass spectra of peptides containing C206 and C215 of reduced ($-H_2O_2$, *upper panels*) and oxidized ($+H_2O_2$, *lower panels*) OxyR2 were indicated; ▼, m/z = 1541.7, a peptide with alkylated C206 and C215; ▽, m/z = 1425.7, a peptide with disulphide-bonded C206 and C215.

(Fig. 5A, upper panel). In the oxidized OxyR2, the peptides containing alkylated C49, C91, C104 and C114 were still detectable (Fig. 5A, lower panel). However, the peptide containing alkylated C206 and C215, of which the theoretical monoisotopic mass is 1541.7, disappeared in the presence of H_2O_2 (Fig. 5A, lower panel, and Fig. 5B). If C206 and C215 formed a disulphide bond and thus not alkylated, the monoisotopic mass of the peptide would be 1425.7. Indeed, a peptide with a mass of 1425.7 was specifically detected in the oxidized OxyR2 (Fig. 5A, lower panel, and Fig. 5C), indicating that OxyR2 was oxidized by forming a disulphide bond between C206 and C215 under oxidative stress. A peptide containing alkylated C29 was not detected in either reduced or oxidized OxyR2s, suggesting that C29 was unable to be alkylated under the experimental conditions. These combined results (Figs 2–5) indicated that OxyR2 is an OxyR-type regulator that senses oxidative stress by means of a reversible disulphide bond formation between C206 and C215 and regulates the expression of the antioxidant defence genes (Åslund *et al*., 1999; Zheng *et al*., 2001).

Only the oxidized OxyR2 can activate expression of Prx2

To determine the role of each cysteine further, the activities of the wild-type and mutant OxyR2s *in vivo* were compared by measuring the Prx2 production in the cells grown aerobically (Fig. 6A). Prx2 was produced without exposure to H_2O_2 in the wild type as observed in Northern blot analysis (Fig. 2A). Similar levels of Prx2 were produced in the cells harbouring plasmids expressing mutant OxyR2s having C29S, C49S, C91S, C104S and C114S mutations, indicating that the C29, C49, C91, C104 and C114 residues are not critical for the activity of OxyR2 (Fig. 6A). In contrast, expression of Prx2 was reduced significantly in the cells harbouring pDY1104 expressing OxyR2-C206S, a reduced form of OxyR2 (Fig. 6A). Since the cellular level of the OxyR2-C206S, determined by Western blot analysis, was not significantly different from that of the wild-type OxyR2, the reduction of Prx2 expression resulted from reduced activity rather than the amount of OxyR2-C206S in the cells. These results supported our previous assumption that C206 is a sensing cysteine oxidized upon exposure to H_2O_2 and indicated that only the oxidized OxyR2 is active to activate *prx*2. It is noteworthy that OxyR2-C215S was as active as wild-type OxyR2. Since the C206 sensing cysteine of OxyR2-C215S is presumably still oxidized by H_2O_2, but unable to form disulphide bond with C215, this result indicated that oxidation of C206 alone, as well as disulphide bond formation, would be enough for the activity of OxyR2.

The activities of the wild-type and mutant OxyR2s *in vivo* were compared by measuring the *prx*2 transcription

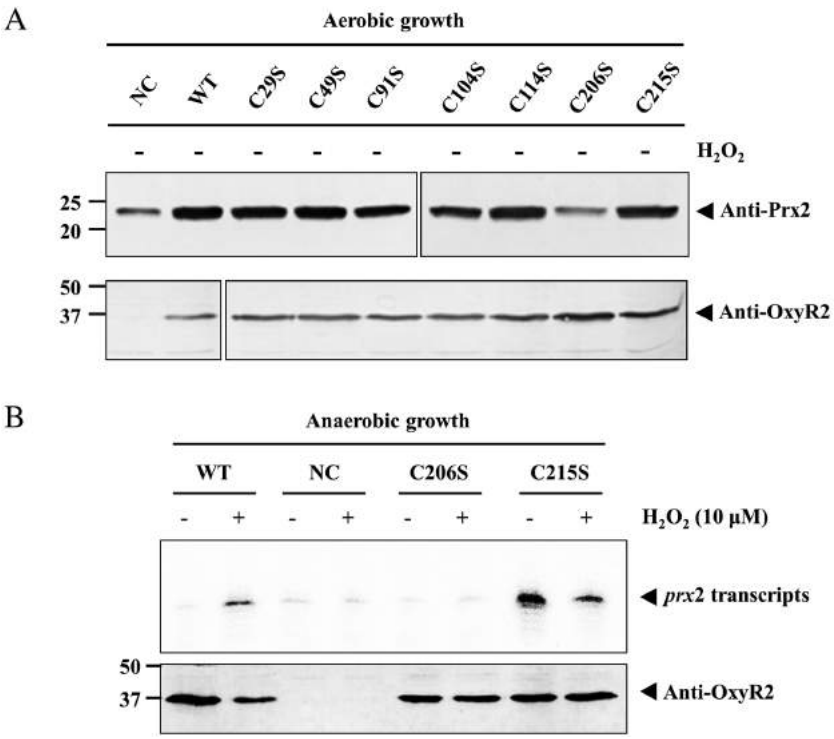

Fig. 6. Effects of the mutations of seven cysteines on the OxyR2 activity.
A. The *oxyR*2 mutant containing plasmids expressing wild-type (WT) or mutant OxyR2s (each of seven cysteines was mutated to serine as indicated) were grown aerobically to an A_{600} of 0.5. Total proteins were resolved on SDS-PAGE and immunoblotted using the rabbit anti-Prx2 antibody (*upper panel*) and anti-OxyR2 antibody (*lower panel*). The protein size markers (Precision Plus Protein Standards; Bio-Rad Laboratories) are shown in kilodaltons and OxyR2 and Prx2 proteins (*arrows*) are indicated.
B. The *oxyR*2 mutant containing plasmids expressing wild-type (WT) or mutant OxyR2s (C206 or C215 was mutated to serine as indicated) were grown anaerobically to an A_{600} of 0.3. Total RNAs were isolated from the cultures treated (+) or not treated (–) with 10 μM H_2O_2 for 30 s and used for the primer extension analysis. Total proteins were resolved on SDS-PAGE and immunoblotted using the rabbit anti-OxyR2 antibody (*lower panel*). For both panels, NC, negative control (the *oxyR*2 mutant containing pJH0311).

in the cells grown anaerobically (Fig. 6B). Primer extension analyses were used to measure the *prx*2 transcript, and the same sequencing ladders presented later in this study (Fig. 9A) were used to determine the transcription start site of *prx*2. The *prx*2 transcript was not detected in the cells harbouring pDY1025 expressing the wild-type OxyR2 without exposure to H_2O_2, whereas the *prx*2 transcript appeared when the cells were exposed to H_2O_2. In contrast, the *prx*2 transcript was not detectable in the cells harbouring pDY1104 expressing OxyR2-C206S regardless of exposure to H_2O_2, confirming that oxidation of C206 is essential for the activity of OxyR2 (Fig. 6B). The cellular level of OxyR2-C206S was not significantly different from that of the wild-type OxyR2, indicating that the loss of OxyR2-C206S activity is due to the inactive conformation of the protein and oxidation and reduction of OxyR2 is associated with a conformational change. However, it is noteworthy that the *prx*2 transcription in the cells expressing OxyR2-C215S was comparable to that of the cells expressing wild-type OxyR2 and was constitutive regardless of exposure to H_2O_2. These results indicated that mutation of C215 probably led to the conformational change of OxyR2-C215S to an active form, albeit by unknown mechanisms (Fig. 6B).

OxyR2 senses lower levels of H_2O_2 *than OxyR1*

In order to identify the minimum concentrations of H_2O_2 required for the oxidation of OxyRs, strains expressing the wild-type OxyR2 and OxyR1 were grown anaerobically and exposed to various concentrations of H_2O_2 (Fig. 7A and B). Most OxyR2 and OxyR1 were reduced in the cells unexposed to H_2O_2 (negative control), and their oxidation occurred upon exposure to increasing concentrations of H_2O_2 as evidenced by the approximately 1 kDa decrease in molecular size of the alkylated OxyRs (Fig. 7A and B). Oxidation of OxyR2 occurred initially upon exposure to 0.5 μM H_2O_2 within 30 s (Fig. 7A). In contrast, OxyR1 was not oxidized until exposed to 5 μM H_2O_2 (Fig. 7B). From these results, it was apparent that OxyR2 is oxidized by sensing lower levels of H_2O_2 compared to OxyR1. Same experimental conditions were used to determine the activities of OxyR2 and OxyR1 by measuring the transcript of *prx*2 and *prx*1 respectively (Fig. 7C and D). Northern blot analyses demonstrated that the transcript of *prx*2 was apparent when the strains were exposed to exogenous H_2O_2 exceeding 0.1 μM (Fig. 7C). In contrast, transcription of *prx*1 occurred poorly until exposed to 5 μM H_2O_2 (Fig. 7D). These results confirmed our previous observation that OxyR2 is activated by sensing lower levels of H_2O_2. This discrete expression pattern of the Prxs implied that the two OxyRs have distinct roles in protecting the bacteria from oxidative stress of different levels and from different sources. OxyR2 protects bacteria from endogenous H_2O_2 by activating the expression of Prx2 effective for detoxifying low levels of H_2O_2, whereas OxyR1 protects the bacteria from exogenous

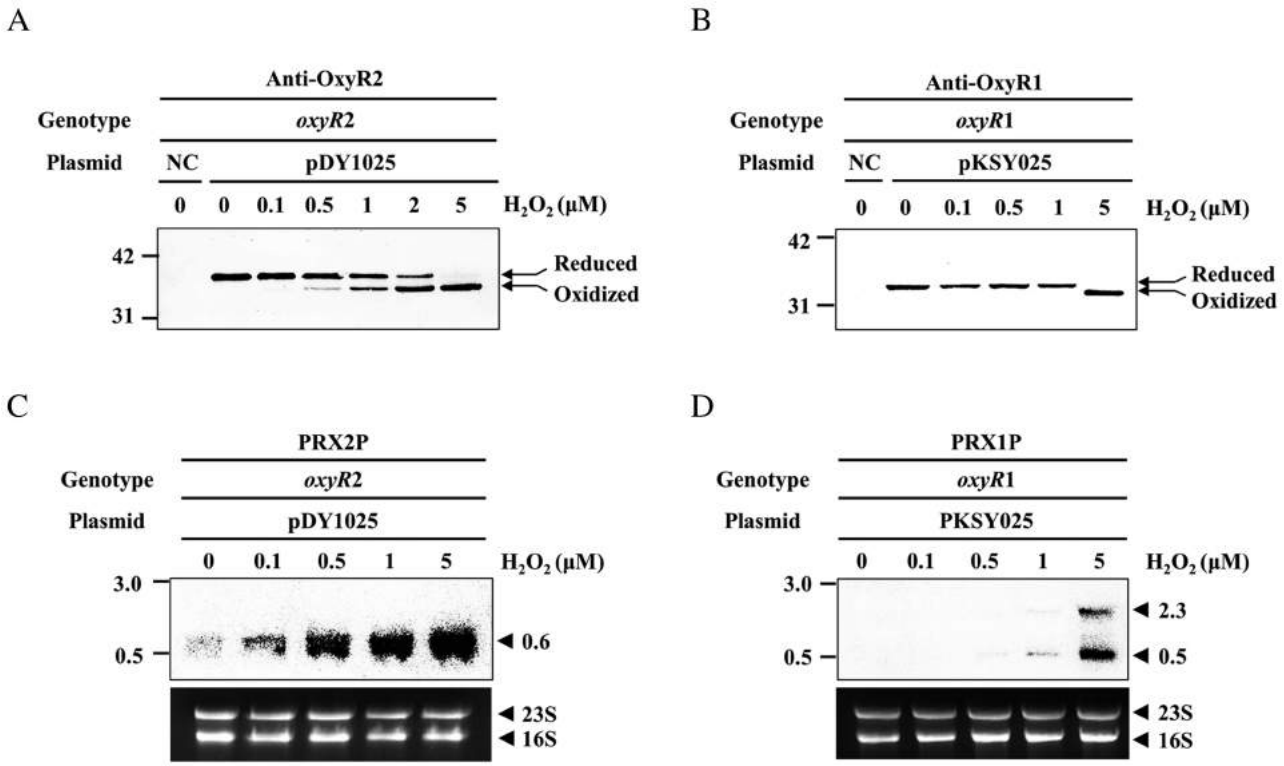

Fig. 7. Minimum concentrations of H_2O_2 to oxidize OxyR2 and OxyR1. Cultures were grown anaerobically to an A_{600} of 0.3. For A and B, the *oxyR*2 mutant containing pDY1025 expressing wild-type OxyR2 (A) and the *oxyR*1 mutant containing pKSY025 expressing wild-type OxyR1 (B) were treated with increasing concentration of H_2O_2 for 30 s, precipitated with TCA, and incubated with fresh AMS buffer for 1 h at 37°C for alkylation of free-thiols in cells. Alkylated proteins were resolved by non-reducing SDS-PAGE and immunoblotted using the rabbit anti-OxyR2 (A) and anti-OxyR1 (B) antibodies. The protein size marker (Precision Plus Protein Standards; Bio-Rad Laboratories) are shown in kilodaltons and the two states (reduced- and oxidized) of OxyR2 and OxyR1 proteins (*arrows*) are indicated. *oxyR*2, *oxyR*2 mutant; *oxyR*1, *oxyR*1 mutant; NC, negative control (pJH0311). For C and D, the *oxyR*2 mutant containing pDY1025 (C) and the *oxyR*1 mutant containing pKSY025 (D) were treated with increasing concentration of H_2O_2 for 30 s. Total RNAs were isolated, resolved and hybridized with [α-^{32}P]-labelled DNA probe corresponding to the internal coding regions of *prx*2 (PRX2P) and *prx*1 (PRX1P). The RNA size markers (0.5–10 kb RNA Ladder; Invitrogen) and *prx*1 and *prx*2 transcripts are shown in kilobases.

H_2O_2 by activating the expression of Prx1 effective for scavenging high levels of H_2O_2.

OxyR2$_{5CA}$ activates prx2 expression in vivo

To further understand the mechanisms of OxyR2 for the activation of *prx*2, OxyR2 was purified and tested to determine whether or not it folded properly *in vitro*. The purified OxyR2 protein was present as a monomer under reducing conditions, while it turned into oligomers with larger molecular sizes under non-reducing conditions (Fig. 8A). From the results, we assumed that cysteines of an OxyR2 could form intermolecular disulphide bonds with cysteines from other OxyR2 molecules *in vitro*, and result in oligomerization of the protein. Therefore, a mutant OxyR2, in which all five of the non-critical cysteine residues (C29, C49, C91, C104 and C114) were replaced with alanines, was constructed and named OxyR2$_{5CA}$. The purified OxyR2$_{5CA}$ did not form oligomers *in vitro* under non-reducing conditions (Fig. 8A).

To determine whether or not OxyR2$_{5CA}$ is active or not *in vivo*, the *oxyR*2 mutant containing plasmids expressing OxyR2$_{5CA}$ or wild-type OxyR2 were grown aerobically and the *prx*2 expression was compared. The results of Fig. 8B revealed that the expression level of *prx*2 in the strain expressing OxyR2$_{5CA}$ did not significantly differ from that of the strain expressing wild-type OxyR2. Furthermore, the cellular level of OxyR2$_{5CA}$ was similar to that of the wild-type OxyR2 (Fig. 8B). When compared again using the cells grown anaerobically, the activities of OxyR2 and the OxyR2$_{5CA}$ to activate *prx*2 did not significantly differ (Fig. S2A). Furthermore, OxyR2$_{5CA}$-C206S was unable to activate *prx*2 in aerobic conditions *in vivo* (Fig. S2B) as was OxyR2-C206S (Fig. 6A), indicating that the C206S mutation caused the same effects on the functions of both OxyR2 and OxyR2$_{5CA}$ proteins. These combined results indicated that OxyR2$_{5CA}$ and OxyR2 are functionally similar and the effects of collectively all 5 cysteine mutations together on the activity the OxyR2 were marginal and not significant. Therefore, purified OxyR2$_{5CA}$, instead

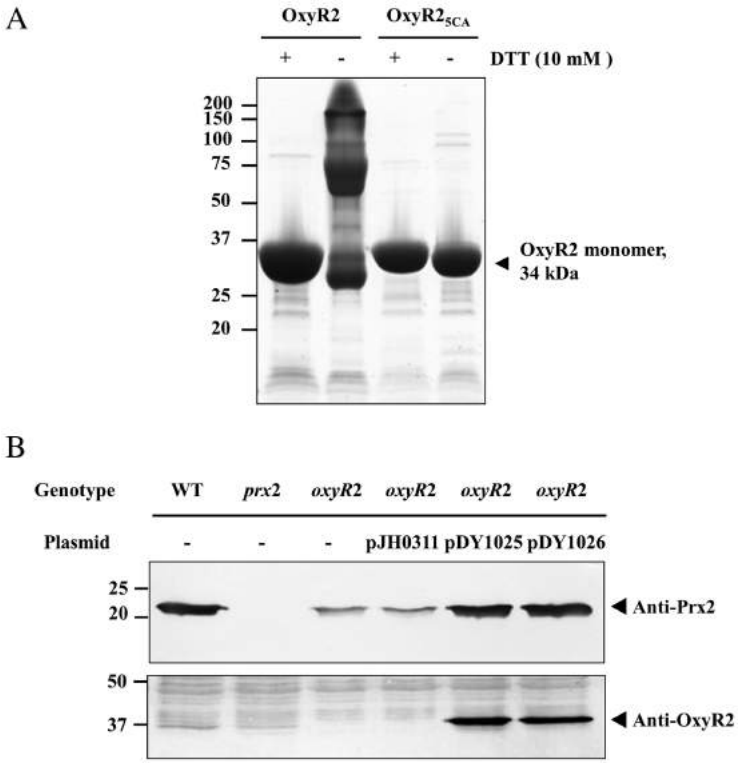

Fig. 8. Construction of OxyR2$_{5CA}$ and its activity *in vivo*.
A. Purified OxyR2 and OxyR2$_{5CA}$ proteins were resolved on SDS-PAGE with (+) or without (–) 10 mM DTT as indicated.
B. Cultures of the wild type (WT), *prx*2 mutant, *oxyR*2 mutant, *oxyR*2 mutant containing pDY1025 expressing wild-type OxyR2 and pDY1026 expressing OxyR2$_{5CA}$ were grown aerobically to an A_{600} of 0.5 as indicated. Total proteins were isolated, resolved on SDS-PAGE, and immunoblotted using the rabbit anti-Prx2 (*upper panel*) and anti-OxyR2 (*lower panel*) antibodies. For both panels, the protein size markers (Precision Plus Protein Standards; Bio-Rad Laboratories) and OxyR2 and Prx2 proteins (*arrows*) are shown in kilodaltons.

of OxyR2, was used *in vitro* hereafter to further analyse the molecular mechanisms of the protein to activate the *prx*2 expression. Indeed, OxyR$_{4CA}$, in which all four of the non-critical cysteine residues were replaced with alanines, was constructed previously and used generally for analyses of structure and activities *Ec*OxyR *in vitro* (Zheng *et al*., 1998; Choi *et al*., 2001; Lee *et al*., 2004).

Identification of the promoter sequences for prx2

In order to map the promoter of *prx*2, the transcription start site of *prx*2 was determined by a primer extension analysis. A single reverse transcript was produced from primer extension of RNA isolated from wild type grown aerobically to an A_{600} of 0.5 (Fig. 9A). The 5′ end of the *prx*2 transcript was located 69 bp upstream of the translational initiation codon of *prx*2 and subsequently designated +1 (Fig. 9B). The putative promoter constituting this transcription start site was named P_{prx2}. Using different sets of primers, no other transcription start sites were identified by primer extension analyses (data not shown). This transcription start site was the same transcription start site previously determined by primer extension of the RNA isolated from the cells grown anaerobically and exposed to H_2O_2 (Fig. 6B). This indicated that a single promoter, P_{prx2}, is used for the transcription of *prx*2 regardless of exposure of the cells to oxidative stress. The sequences for –10 and –35 regions of P_{prx2} were assigned on the basis of similarity to consensus sequences of the *E. coli* σ^{70} promoter (Fig. 9B).

OxyR2 directly binds to P_{prx2}

The 260 bp labelled DNA probe encompassing the *prx*2 promoter region was incubated with increasing amounts of OxyR2$_{5CA}$ and then subjected to electrophoresis. As seen in Fig. 10A, the addition of OxyR2$_{5CA}$ resulted in a concentration-dependent ladder of two retarded bands, indicating that at least two binding sites for OxyR2$_{5CA}$ would be present within the *prx*2 promoter region. The binding of OxyR2$_{5CA}$ was also specific because assays were performed in the presence of 200 ng of poly(dI-dC) (Sigma, St Louis, MO) as a nonspecific competitor. In a second electrophoretic mobility shift assay (EMSA), the same but unlabelled 260 bp DNA fragment was used as a self-competitor to confirm the specific binding of OxyR2$_{5CA}$. The unlabelled 260 bp DNA competed for the binding of OxyR2$_{5CA}$ in a dose-dependent manner (Fig. 10A), confirming that OxyR2$_{5CA}$ binds specifically to the DNA. The results indicated that OxyR2$_{5CA}$ is air-oxidized properly and binds specifically to the *prx*2 promoter region. In similar DNA-binding assays, OxyR2$_{5CA}$-C206S and OxyR2$_{5CA}$-C215S which are unable to form disulphide bonds, also displayed specific binding to the *prx*2 regulatory region (Fig. 10B and C). Based on the concentrations of OxyR2 proteins that were required to

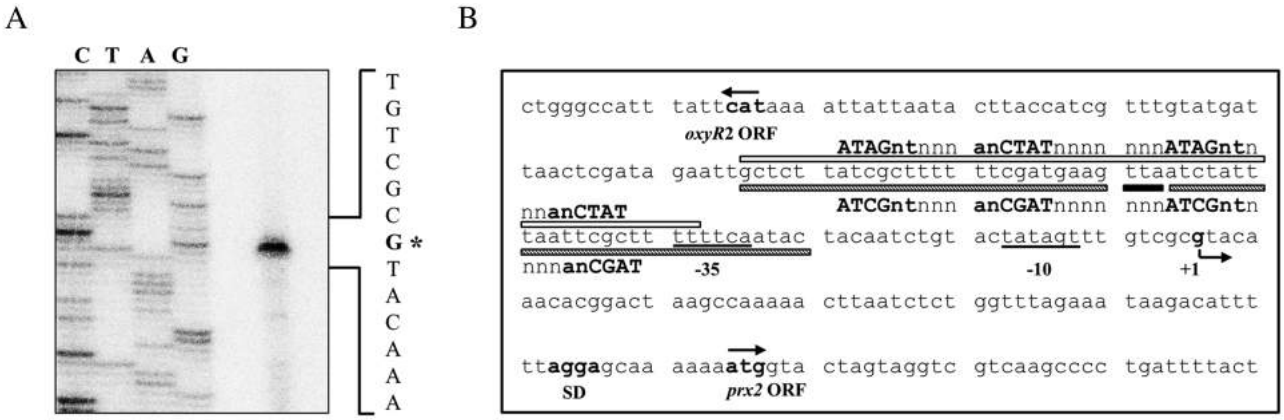

Fig. 9. Transcription start site and sequences of the *prx*2 promoter region.
A. The transcription start site was determined by primer extension of the RNA isolated from the wild type grown aerobically to an A_{600} of 0.5. Lanes C, T, A and G represent the nucleotide sequencing ladders of pOH058. The *asterisk* indicates transcription start site for P_{prx2}.
B. The transcription start site of P_{prx2} is indicated by a *bent arrow* and the positions of the putative –10 and –35 regions are *underlined*. The sequences for binding of oxidized OxyR2 (*a white box*) and for binding of reduced OxyR2 (*shaded boxes*) determined later in this study (Fig. 11) are presented. The nucleotides showing enhanced cleavage are indicated by *a black box*. The consensus sequences for binding of oxidized *Ec*OxyR and putative sequences for binding of oxidized OxyR2 are respectively indicated *above* and *below* the *V. vulnificus* DNA sequence. ATAGnt *Ec*OxyR binding motif and ATCGnt OxyR2 binding motif predicted from this study are shown in *boldface*. The ATG translation initiation codons and the putative ribosome binding site (SD) are also indicated in *boldface*. n, any nucleotides.

retard 50% of the labelled probe, the dissociation binding constants (K_d) for $OxyR2_{5CA}$ and $OxyR2_{5CA}$-C206S were not significantly different (approximately 50 and 40 nM respectively) (Fig. 10D). These results indicated that OxyR2, oxidized or reduced, were able to bind to their operator within the *prx*2 promoter with comparable affinity. However, $OxyR2_{5CA}$-C215S exhibited the K_d value of approximately 170 nM, indicating that the binding affinity of $OxyR2_{5CA}$-C215S to *prx*2 promoter is significantly lower than those of $OxyR_{5CA}$ and $OxyR_{5CA}$-C206S.

Identification of the OxyR2 binding site

The oxidized *Ec*OxyR is known to binds as a tetramer to the consensus sequence consisting of four ATAGnt elements separated by a helical turn (Toledano *et al*., 1994). To determine the OxyR2 binding site in the *prx*2 promoter region, DNase I protection assays were performed using the same 260 bp DNA fragment used for the EMSA. As shown in Fig. 11A, a region extending from –80 and to –33 relative to the transcription start site of P_{prx2} was clearly protected by $OxyR2_{5CA}$. The predicted binding site for $OxyR2_{5CA}$, centred at –56.5, indicated that the oxidized OxyR2 is a class I activator interacting directly with RNA polymerase (α-C terminal domain) in a similar manner to the oxidized *Ec*OxyR (Tao *et al*., 1993). Inspection of the sequences of the protected region revealed low levels of matches with the consensus *Ec*OxyR-binding sequence. Instead, the putative OxyR2 binding sequences contained four repeats of the ATCGnt element, rather than the ATAGnt element, spaced by a helical turn and stretched in the twofold dyad symmetry (Fig. 9B). These indicated that OxyR2 also binds to DNA as a tetramer but has a DNA binding specificity distinct from that of *Ec*OxyR. Similar DNase I protection assays were performed with $OxyR2_{5CA}$-C206S, the reduced form of OxyR2 (Fig. 11B). The binding sequences for $OxyR_{5CA}$-C206S were elongated compared to those for $OxyR_{5CA}$ and separated into two regions, extending from –26 to –52 and from –56 to –80. Several nucleotides (–53 to –55) of the sequences revealed enhanced cleavages, indicating that binding of the reduced OxyR2 altered the configuration of the DNA of P_{prx2} (Figs 9B and 11B). These indicated that the oxidized and reduced OxyR2 also adopt different conformational states leading to changes in the DNA binding contacts, as observed in *Ec*OxyR (Toledano *et al*., 1994; Choi *et al*., 2001). Interestingly, $OxyR2_{5CA}$-C215S bound to the sequences identical to those for binding of $OxyR2_{5CA}$ (Fig. 11C). This is consistent with our previous observation that OxyR2-C215S is able to activate P_{prx2} (Fig. 6).

Effects of the oxyR2 mutation on the virulence and growth rate of V. vulnificus

In an effort to understand the role of OxyR2 in *V. vulnificus* pathogenesis, the activities of LDH released from the INT-407 cells infected with the wild-type and *oxyR*2 mutant strains were compared (Fig. 12A). The *oxyR*2 mutant exhibited significantly lower LDH-releasing activity than the wild type strain when the multiplicity of infection

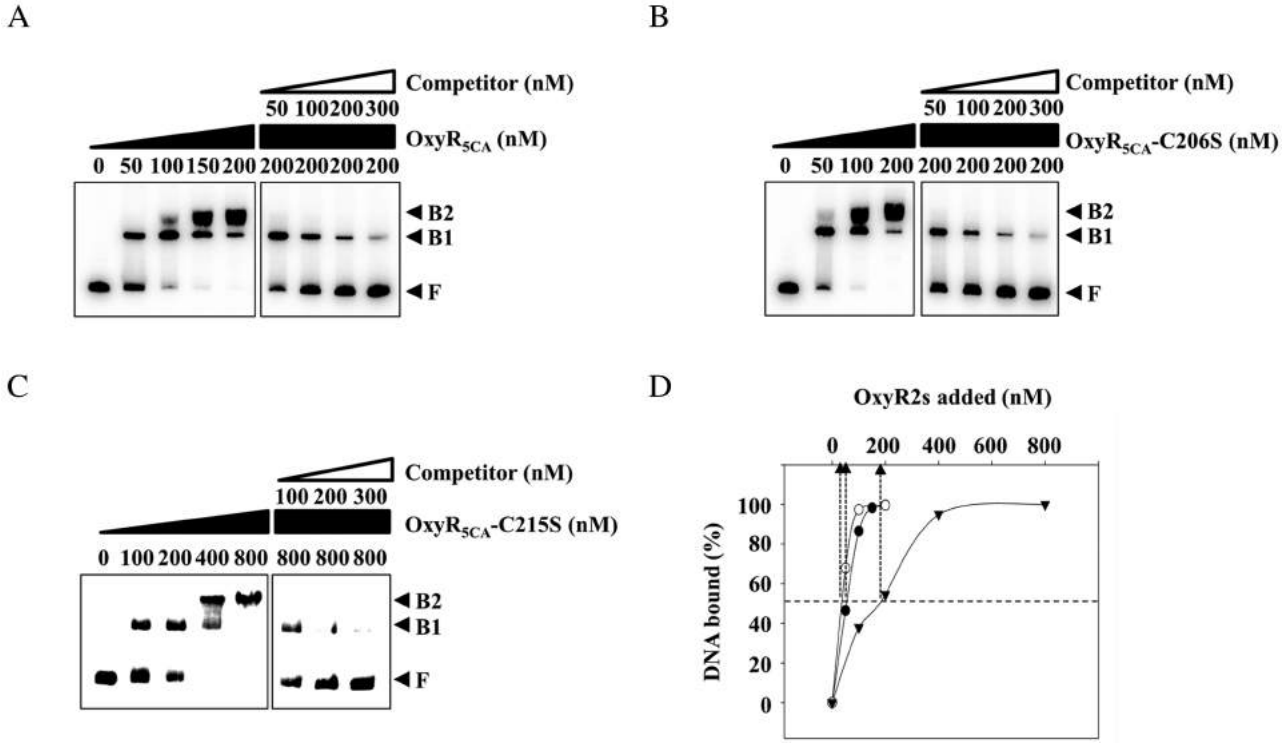

Fig. 10. Specific binding of OxyR2$_{5CA}$, OxyR2$_{5CA}$-C206S and OxyR2$_{5CA}$-C215S to P$_{prx2}$.
A–C. A 260 bp DNA fragment of the upstream region of P$_{prx2}$ was radioactively labelled and then used as a probe DNA. The radiolabelled probe DNA (5 nM) was mixed with increasing amounts of OxyR2$_{5CA}$ (A), OxyR2$_{5CA}$-C206S (B) and OxyR2$_{5CA}$-C215S (C) as indicated. For competition analysis, the same but unlabelled DNA fragment was used as a self-competitor DNA. Various amounts of the self-competitor DNA were added to a reaction mixture containing the 5 nM labelled DNA prior to the addition of 200 nM OxyR2$_{5CA}$ (A), 200 nM OxyR2$_{5CA}$-C206S (B) and 800 nM OxyR2$_{5CA}$-C215S (C). F, free unbound DNA; B1 and B2, OxyR2-bound DNA.
D. The relative affinities of OxyR2$_{5CA}$, OxyR2$_{5CA}$-C206S and OxyR2$_{5CA}$-C215S for the upstream region of P$_{prx2}$ were compared using the data from A, B and C respectively. The concentration of bound DNA was calculated and plotted against the concentration of the proteins added. Each *arrow* points to the position of half-maximal binding corresponding to the K_d. ●, OxyR2$_{5CA}$; ○, OxyR2$_{5CA}$-C206S; ▼, OxyR2$_{5CA}$-C215S.

(moi) was up to 30, indicating that OxyR2 is important for *V. vulnificus* to infect and injure host cells. Complementation of the *oxyR*2 gene in the *oxyR*2 mutant with a functional *oxyR*2 gene (pDY1025) restored the LDH-releasing activity to levels comparable to wild-type levels (Fig. 12A). To examine whether the reduced cytotoxicity of the *oxyR*2 mutant resulted from defects in its growth, we compared the growth rate of the *oxyR*2 mutant with that of the wild type. The growth rate of the *oxyR*2 mutant in minimal essential medium with 1% fetal bovine serum was not significantly different from that of the wild type (data not shown). During infection, however, the growth rate of the *oxyR*2 mutant in the supernatant of the INT-407 cells was significantly lower than that of the wild type and complemented strains. The *oxyR*2 mutant was unable to grow for as long as 1.5 h during infection while the wild type and the complemented strains showed about threefold increase in colony-forming units (cfu) (Fig. 12B). It has been reported that the host epithelial cells infected with *V. vulnificus* generate ROS (Chung *et al*., 2010). Therefore, it is conceivable that growth defect of the *oxyR*2 mutant during infection resulted from the decreased *prx*2 expression due to the lack of OxyR2. These results suggest that the decreased virulence of the *oxyR*2 mutant in tissue culture likely resulted from its growth defect, indicating that OxyR2 could play a role in the pathogenesis of *V. vulnificus* by assuring survival and multiplication during infection.

Discussion

*Ec*OxyR is a redox-sensitive global regulator which activates the expressions of over 20 antioxidant defence genes under oxidative stress and represses its own expression during normal aerobic growth conditions (Tao *et al*., 1991; Zheng *et al*., 2001). This study presented OxyR2, another OxyR of *V. vulnificus*, that activates the expression of Prx2 during normal aerobic growth without exposure to exogenous H_2O_2 (Fig. 2A). Prx2 seems effective for the reduction of low levels of H_2O_2 formed internally rather than high levels of H_2O_2 provided exogenously (Bang *et al*., 2012). This indicated that OxyR2 is

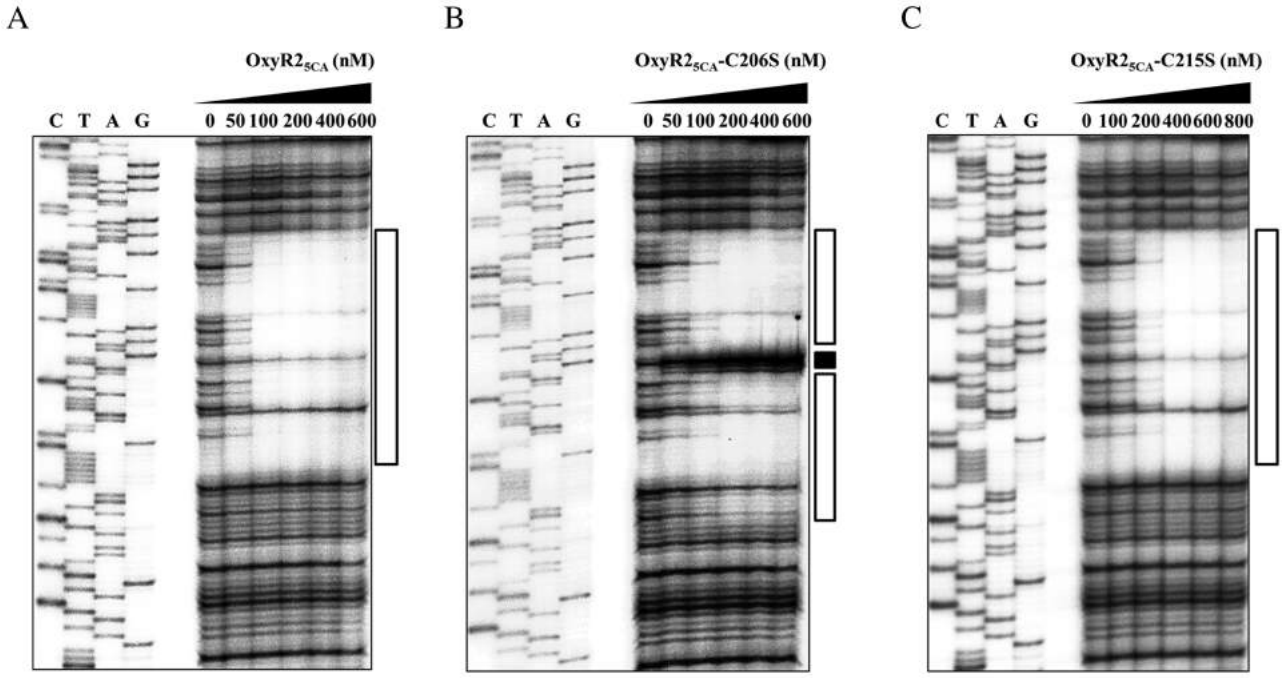

Fig. 11. Sequences for binding of OxyR2$_{5CA}$, OxyR2$_{5CA}$-C206S and OxyR2$_{5CA}$-C215S to P_{prx2}. A 260 bp DNA fragment of the upstream region of P_{prx2} was radioactively labelled and then used as a probe DNA. The radiolabelled probe DNA (25 nM) was incubated with increasing amounts of OxyR2$_{5CA}$ (A), OxyR2$_{5CA}$-C206S (B) and OxyR2$_{5CA}$-C215S (C) as indicated, and then digested with DNase I. The regions protected by OxyR2$_{5CA}$, OxyR2$_{5CA}$-C206S and OxyR2$_{5CA}$-C215S are indicated by *open boxes*, whereas the nucleotides showing an enhanced cleavage in the presence of OxyR2$_{5CA}$-C206S are indicated by a black box. Lanes C, T, A and G represent the nucleotide sequencing ladders of pKSY036.

constitutively expressed in the cells during aerobic growth, and becomes the residential redox-sensitive regulator contributing to the survival of the bacteria by retaining endogenous H_2O_2 accumulation within the safe limits. Consistent with this, OxyR2 is more efficient in sensing trace amounts of H_2O_2 than is OxyR1 (Fig. 7). Furthermore, the present study revealed that the *oxyR*2 mutant exhibited significantly reduced cytotoxicity and lower growth rate than the wild-type strain in tissue culture, indicating that OxyR2 could play a role in the

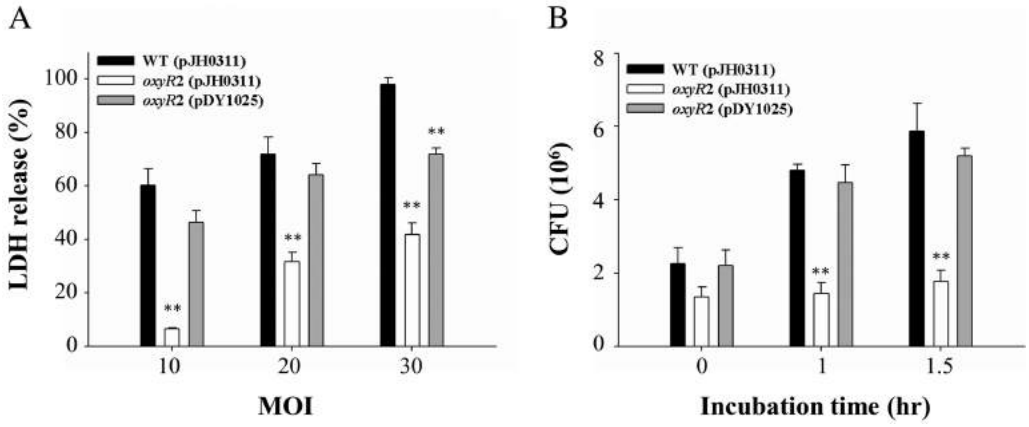

Fig. 12. Effect of *oxyR*2 mutation on virulence of *V. vulnificus* toward INT-407 cells and growth rate during infection.
A. INT-407 cells were infected with the *V. vulnificus* strains at various moi for 1.5 h. The cytotoxicity was determined by an LDH release assay and expressed using the total LDH released from the cells completely lysed by 1% Triton X-100 as 100%.
B. Growth of the strains during the infection of INT-407 cells was monitored. The strains were used to infect the INT-407 cells at an moi of 20. The bacterial cells in the supernatant were determined by counting cfu on LBS agar plates at time intervals as indicated. Error bars represent the SEM. $^{**}P < 0.005$ relative to groups infected with the wild type at each condition. WT (pJH0311), wild type; *oxyR*2 (pJH0311), *oxyR*2 mutant; *oxyR*2 (pDY1025), complemented strain.

pathogenesis of *V. vulnificus* by detoxifying H_2O_2, likely generated by host cells, during infection.

As observed in *Ec*OxyR, it is most likely that sensing of H_2O_2 by OxyR2 and OxyR1 could occur via oxidation of the putative sensing cysteines C206 and C199 respectively. Structural analysis of *Ec*OxyR proposed that the basic R266 residue makes close contact with C199 and provides a positively charged environment enhancing the reactivity of the cysteine sulphur (Choi *et al*., 2001). The reactivity of the cysteine sulphur is enhanced when it is deprotonated to thiolate anion ($-S^-$), which is more nucleophilic and reacts faster with H_2O_2 than the protonated form (-SH) (Netto *et al*., 2007). When the secondary structure of the proteins were predicted using Phyre2 (http://www.sbg.bio.ic.ac.uk/phyre2) (Kelley and Sternberg, 2009) and visualized using PyMOL v1.7 (http://www.pymol.org), identical R residues (R274 of OxyR2 and R266 of OxyR1) were predicted to contact with C206 of OxyR2 and C199 of OxyR1 (Fig. S3). However, the C206 of OxyR2 is neighboured additionally by the positively charged K203, whereas C199 of OxyR1 is neighboured by the negatively charged D196 (Figs 1 and S3). Therefore, one plausible explanation for the enhanced sensitivity of OxyR2 to H_2O_2 is that the additional charge interaction between C206 and K203 further stabilize the thiolate anion form of C206, lowering the pKa of the cysteine sulphur and enhancing its reactivity to H_2O_2.

OxyR is a member of the LysR family of transcriptional activators and binds to DNA as a tetramer (Toledano *et al*., 1994). The oxidized *Ec*OxyR binds four adjacent major grooves containing four repeats of the ATAGnt element spaced respectively by a helical turn, whereas the reduced *Ec*OxyR binds to two pairs of major grooves separated by a helical turn (Toledano *et al*., 1994). The binding sequences for the air-oxidized $OxyR2_{5CA}$ consist of four ATCGnt elements spaced by a helical turn and shows a twofold dyad symmetry (Figs 9B and 11A). The binding sequences for $OxyR_{5CA}$-C206S, the reduced form of OxyR2, was elongated compared with those for $OxyR_{5CA}$ and separated into two regions by a helical turn and an additional ATCGnt element was found in the elongated sequences (Figs 9B and 11B). All these observations lead us to suggest that OxyR2 binds to DNA as a tetramer with a pattern similar to that of *Ec*OxyR. The ATCGnt element for binding of OxyR2 that is noticeably distinct from that of *Ec*OxyR (ATAGnt) is presumably attributed to the difference found in the residues of the DBD of the two proteins (Fig. 1B). However, no OxyR2-binding sequence, other than P_{prx2}, is presently available and data are insufficient to evaluate whether ATCGnt is indeed a consensus element for the binding of OxyR2. Additional work is needed to gain insight into the conserved binding pattern and specificity of OxyR2 to its target DNAs.

Prx2 expression of the *oxyR*2 mutant harbouring pDY1104 expressing OxyR2-C206S, the reduced form of OxyR2, was not significantly different from that of the mutant harbouring pJH0311 (negative control) (Fig. 6A). This indicated that P_{prx2} activity *in vivo* was not repressed by OxyR2 under reducing conditions, albeit the binding site *in vitro* for $OxyR2_{5CA}$-C206S slightly overlapped with the RNAP binding site (–35 region) (Fig. 9B). Although OxyR2-C206S and OxyR2-C215S are not able to form disulphide bonds, their oxidation status could be different. OxyR2-C206S is not able to sense H_2O_2 and locked in the reduced form, whereas OxyR2-C215S can be oxidized by H_2O_2 via oxidation of sensing cysteine C206. Interestingly, OxyR2-C215S was able to activate Prx2 expression (Fig. 6A), and the activation was constitutive and not dependent on exposure to H_2O_2 (Fig. 6B). This suggested that the mutation of C215 locked OxyR2 in an active form. Consistent with this, the sequences for binding of $OxyR2_{5CA}$-C215S were identical to those of $OxyR2_{5CA}$ (Fig. 11C). However, increased amount of $OxyR2_{5CA}$-C215S was required for binding to P_{prx2} (Figs 10D and 11C), indicating that the conformation of OxyR2-C215S would be different from that of the OxyR2 active form. Nevertheless, these results presumably indicated that oxidative modification of the sensing cysteine C206 alone as well as intramolecular disulphide formation was sufficient to activate OxyR2. This direct activation via modification of sensing cysteine alone was also observed in *Ec*OxyR (Kim *et al*., 2002).

In summary, this study presented the two OxyRs of *V. vulnificus* that sense different ranges of oxidative stress by means of the reversible oxidation of specific cysteine residues and activate the transcription of the distinct antioxidant defence genes. OxyR2 senses low levels of H_2O_2 and activates Prx2, a residential scavenger of peroxides generated endogenously, whereas OxyR1 (a homologue of *Ec*OxyR) senses high levels of H_2O_2 and activates Prx1, an occasional scavenger of peroxides encountered exogenously. To our knowledge, this is the first report on the coexistence of two OxyRs leading to the discrete expression of the distinct antioxidants in a single bacterium. This discrete expression of antioxidants effective for detoxifying different ranges of H_2O_2 could provide an evolutionary advantage by protecting bacteria from oxidative stress of different sources. Consistent with this, a search for homologues to OxyR2 in bacterial genomes revealed many other bacterial species that seem to be equipped with both OxyR homologues, including *Aeromonas* sp., *Aliivibrio* sp., *Grimontia* sp., *Photobacterium* sp., *Vibrionales* sp. as well as *Vibrio* sp. (Table 1). Therefore, the coexistence of the two OxyRs seems as a part of the bacterial nature, not limited to only *V. vulnificus*.

Table 1. Coexistence of OxyR1 and OxyR2 homologues among bacteria.[a,b]

Species and strain	OxyR1 homologues			OxyR2 homologues		
	NCBI Accession Number	Identity (%)[c]		NCBI Accession Number	Identity (%)[c]	
		E	*V*		*E*	*V*
Vibrio sp.						
V. vulnificus MO6-24/O	ADV85339	63	34	ADV87476	37	100
V. cholera O395	ABQ20950	64	32	ABQ20012	37	86
V. parahaemolyticus RIMD 2210633	BAC61015	63	31	BAC58844	36	90
V. harveyi HY01	EDL67529	62	32	EDL68002	38	92
V. splendidus ATCC 33789	EGU45638	63	33	EGU42017	37	91
Aeromonas sp.						
A. hydrophila 4AK4	AHE48609	60	36	AHE48818	37	59
A. molluscorum 848	EOD53238	62	36	EOD56234	35	60
A. salmonicida ssp. Pectinolytica 34mel	EQC06131	61	36	EQC06248	36	59
Aliivibrio sp.						
A. fischeri	WP_012534043	66	34	WP_012533880	35	82
A. salmonicida LFI1238	CAQ80398	67	34	CAQ80124	35	82
Grimontia sp.						
G. hollisae CIP 101886	EEY73719	70	32	EEY72693	33	72
G. sp. AK16	WP_002535235	73	33	WP_002536911	37	71
Photobacterium sp.						
P. angustum S14	EAS63126	71	35	EAS65405	36	74
P. damselae	WP_005302650	72	35	WP_005300827	38	76
P. profundum 3TCK	EAS41863	71	34	EAS40890	35	76
Vibrionales sp.						
V. bacterium SWAT-3	EDK27225	63	33	EDK26251	37	91

a. The OxyR proteins homologous to OxyR1 and OxyR2 in amino acid sequences were singled out from NCBI protein database (NCBI, http://www.ncbi.nlm.nih.gov) using the BLAST (Basic Local Alignment Search Tool, http://blast.ncbi.nlm.nih.gov) program. The OxyR proteins were classified as OxyR1 and OxyR2 homologues if their amino acid sequences share 50% or higher identity to *Ec*OxyR and OxyR2 respectively.
b. All OxyR homologues have the two conserved redox-sensitive cysteines.
c. *E*, identity to *Ec*OxyR; *V*, identity to OxyR2.

Experimental procedures

Strains, plasmids and culture media

The strains and plasmids used in this study are listed in Table 2. Unless noted otherwise, the *V. vulnificus* strains were grown aerobically in Luria–Bertani (LB) medium supplemented with 2.0% (w/v) NaCl (LBS) at 30°C. Anaerobic conditions were obtained by using an anaerobic chamber with an atmosphere of 90% N_2, 5% CO_2 and 5% H_2 (Coy Laboratory Products, Grass Lake, MI). For anaerobic culture, the media was pre-incubated to remove resolved O_2 in the anaerobic chamber, which was verified by adding 0.00001% (w/v) resazurin salt (Sigma) to the media (Kunisaki and Tanji, 2010).

Generation and complementation of oxyR2 or oxyR1 mutants

To inactivate *oxyR*2 *in vitro*, a unique BamHI site was introduced into the open reading frame (ORF) of *oxyR*2 using the PCR-mediated linker-scanning mutation method as described previously (Lim and Choi, 2014). Briefly, pairs of primers OXYR2F1-F and -R for amplification of the 5′ amplicon or OXYR2F2-F and -R for amplification of the 3′ amplicon were designed and used (Table S1). The *oxyR*2 with BamHI site was amplified by PCR using the mixture of both amplicons as the template and OXYR2F1-F and OXYR2F2-R as primers. The *oxyR*2*::nptI* was constructed by insertion of a 1.2 kb *nptI* DNA conferring resistance to kanamycin (Oka *et al*., 1981) into the BamHI site of the PCR products, and ligated with SacI-SalI-digested pDM4 (Milton *et al*., 1996) to form pOH042 (Table 2). Similarly, two-thirds (597 bp of 900 bp) of the *oxyR*1 ORF was deleted *in vitro* using pairs of primers OXYR1F1-F and -R for amplification of the 5′ amplicon or OXYR1F2-F and -R for amplification of the 3′ amplicon (Table S1). The resulting Δ*oxyR*1 was ligated into SpeI–SphI-digested pDM4 to form pJK1122 (Table 2).

E. coli SM10 λ *pir*, *tra* (Miller and Mekalanos, 1988) harbouring either pOH042 or pJK1122 was used as a conjugal donor to *V. vulnificus* MO6-24/O. The conjugation and isolation of the transconjugants were conducted as described previously (Lim and Choi, 2014), and the *V. vulnificus oxyR*2 or *oxyR*1 mutants chosen for further analysis were named OH0703 and JK115 respectively (Table 2). For complementation, pairs of primers, OXYR2C-F and -R (for amplification of *oxyR*2) or OXYR1C-F and -R (for amplification of *oxyR*1), were designed and used (Table S1). The amplified promoterless ORFs of *oxyR*2 and *oxyR*1 were cloned into a broad host-range vector pJH0311 under the *lac* promoter (Goo *et al*., 2006) to create pDY1025 and pKSY025 respectively (Table 2). pDY1025 and pKSY025 were transferred into OH0703 and JK115, respectively, by conjugation as described above. The expression levels of *oxyR*2 from its native promoter were not affected significantly under the con-

Table 2. Bacterial strains and plasmids used in this study.

Strains or plasmids	Relevant characteristics[a]	Reference or source
Bacterial strains		
V. vulnificus		
MO6-24/O	Clinical isolate; virulent	Laboratory collection
OH0505	MO6-24/O with *prx2::nptI*; Km^r	Oh *et al*. (2008)
OH0701	MO6-24/O with *prx1::nptI*; Km^r	Baek *et al*. (2009)
OH0703	MO6-24/O with *oxyR2::nptI*; Km^r	This study
JK115	MO6-24/O with Δ*oxyR*1	This study
E. coli		
DH5α	*supE44 ΔlacU169* (*Φ*80 *lacZ* ΔM15) *hsdR17 recA1 endA1 gyrA96 thi-1 relA1*; plasmid replication	Laboratory collection
SM10 λ *pir*	*thi thr leu tonA lacY supE recA*::RP4-2-Tc::Mu λ*pir*; Km^r; host for π-requiring plasmids; conjugal donor	Miller and Mekalanos (1988)
BL21 (DE3)	F^- *ompT hsdS* (rB^-mB^-) *gal* (DE3)	Laboratory collection
Plasmids		
pDM4	Suicide vector; *ori*R6K; Cm^r	Milton *et al*. (1996)
pOH042	pDM4 with *oxyR2::nptI*; Cm^r, Km^r	This study
pJK1122	pDM4 with Δ*oxyR*1; Cm^r	This study
pJH0311	0.3 kb MCS of pUC19 cloned into pCOS5; Ap^r, Cm^r	Goo *et al*. (2006)
pDY1025	pJH0311 with wild-type *oxyR*2; Ap^r, Cm^r	This study
pKSY025	pJH0311 with wild-type *oxyR*1; Ap^r, Cm^r	This study
pKSY017	pJH0311 with the mutant *oxyR*2 encoding OxyR2-C29S; Ap^r, Cm^r	This study
pKSY018	pJH0311 with the mutant *oxyR*2 encoding OxyR2-C49S; Ap^r, Cm^r	This study
pKSY019	pJH0311 with the mutant *oxyR*2 encoding OxyR2-C91S; Ap^r, Cm^r	This study
pKSY020	pJH0311 with the mutant *oxyR*2 encoding OxyR2-C104S; Ap^r, Cm^r	This study
pKSY021	pJH0311 with the mutant *oxyR*2 encoding OxyR2-C114S; Ap^r, Cm^r	This study
pDY1104	pJH0311 with the mutant *oxyR*2 encoding OxyR2-C206S; Ap^r, Cm^r	This study
pDY1105	pJH0311 with the mutant *oxyR*2 encoding OxyR2-C215S; Ap^r, Cm^r	This study
pDY1026	pJH0311 with the mutant *oxyR*2 encoding $OxyR2_{5CA}$; Ap^r, Cm^r	This study
pDY1027	pJH0311 with the mutant *oxyR*2 encoding $OxyR2_{5CA}$-C206S; Ap^r, Cm^r	This study
pGEM-T Easy	PCR product cloning vector; Ap^r	Promega
pOH058	pGEM-T Easy with a 265 bp fragment of the putative promoter region of *prx*2 ; Ap^r	This study
pKSY036	pGEM-T Easy with a 260 bp fragment of the putative promoter region of *prx*2; Ap^r	This study
pET-28a(+)	His_6–tag fusion protein expression vector; Km^r	Novagen
pDY1001	pET-28a(+) with the wild-type *oxyR*2; Km^r	This study
pDY1014	pET-28a(+) with the mutant *oxyR*2 encoding $OxyR2_{5CA}$; Km^r	This study
pDY1015	pET-28a(+) with the mutant *oxyR*2 encoding $OxyR2_{5CA}$-C206S; Km^r	This study
pDY1016	pET-28a(+) with the mutant *oxyR*2 encoding $OxyR2_{5CA}$-C215S; Km^r	This study
pDY0904	pET-28a(+) with the wild-type *oxyR*1; Km^r	This study

a. Ap^r, ampicillin-resistant; Cm^r, chloramphenicol-resistant; Km^r, kanamycin-resistant.

ditions we used (Fig. S4). This observation is similar to the previous observation that the activity, but not the cellular level, of *Ec*OxyR was affected by the redox state of the growth conditions (Storz *et al*., 1990). It is noteworthy that the difference in the cellular levels of OxyR2, observed when expressed from chromosome (WT in Fig. 8B) and plasmid (*oxyR*2 with pDY1025 in Fig. 8B), did not affect significantly the expression level of Prx2 (Fig. 8B). This result indicated that the increased cellular level of OxyR2 due to the *lac* promoter did not have significant impact on the regulation of *prx*2. When necessary, plasmids carrying mutant *oxyR*2 genes (Table 2) were used to complement OH0703. The resulting complemented strains were used in order to increase the cellular level of the *oxyR*2 (wild type and mutant) or *oxyR*1 transcripts and their gene products for the subsequent transcript and Western blot analyses (Figs 3, 4, 6–8).

RNA purification and transcript analysis

Total cellular RNAs from the cultures grown to the log phase (aerobically to an A_{600} of 0.5 or anaerobically to an A_{600} of 0.3) were isolated using an RNeasy® Mini kit (Qiagen, Valencia, CA) (Bang *et al*., 2012). For Northern blot analysis, reactions were performed according to standard procedures (Sambrook and Russell, 2001) with 10 μg of RNA. The DNA probes, PRX1P and PRX2P, were prepared respectively by labelling DNA fragments containing the *prx*1 and *prx*2 coding regions with [α-^{32}P]-dCTP, and used for hybridization as previously described (Bang *et al*., 2012). For primer extension analysis, a 26-base oligonucleotide primer PRX2PE (Table S1) complementary to the coding region of *prx*2 was end-labelled with [γ-^{32}P]-ATP and added to the RNA. The primer was then extended with SuperScript II RNase H^- reverse transcriptase (Invitrogen). The cDNA products were purified and resolved on a sequencing gel alongside sequencing ladders generated from pOH058 with the same primer PRX2PE (Table 2). The plasmid pOH058 was constructed by cloning the 265 bp *prx*2 upstream region extending from –227 to +38, amplified by PCR using a pair of primers PRX2P01-F and -R, into pGEM-T Easy (Promega, Madison, WI). The Northern blots and primer extension gels were visualized using a phosphorimage analyser (BAS1500, Fuji Photo Film Co. Ltd., Tokyo, Japan).

Protein purification and Western blot analysis

Each ORF of *oxyR*2 and *oxyR*1 was amplified by PCR using pairs of primers, HISOXYR2-F and -R, or HISOXYR1-F and -R respectively (Table S1). The PCR products were ligated into His_6-tagged expression vector, pET-28a (+) (Novagen, Madison, WI), to result in pDY1001 (for OxyR2) and pDY0904 (for OxyR1) (Table 2). His-tagged proteins were expressed in *E. coli* BL21 (DE3), and purified by affinity chromatography according to the manufacturer's procedure (Qiagen). The purified His-tagged OxyR2 and OxyR1 were used to raise rabbit anti-OxyR2 and anti-OxyR1 polyclonal antibodies respectively (AbFrontier, Seoul, South Korea). The anti-Prx2 polyclonal antibody was prepared as described previously (Bang *et al*., 2012). Cultures of the wild type, mutants, and complemented strains grown to the log phase and, when necessary, exposed to H_2O_2, were harvested to isolate total proteins. Proteins (25 μg) were resolved on SDS-PAGE under reducing or non-reducing conditions and immunoblotted as described previously (Lim and Choi, 2014).

In vivo *disulphide bond formation assay*

Cultures were grown anaerobically to an A_{600} of 0.3 or aerobically to an A_{600} of 0.5. The cultures grown anaerobically were exposed either to 10 μM of H_2O_2 for various time intervals or to various concentrations of H_2O_2 for 30 s. To alkylate free thiols in the proteins with 0.5 kDa AMS (Invitrogen), the cells were immediately precipitated with ice-cold TCA, and then the resulting pellets were dissolved in 50 μl of the fresh AMS buffer [15 mM AMS, 1 M Tris, 1 mM EDTA, 0.1% (w/v) SDS, pH 8.0; Lee *et al*., 2004]. After incubation at 37°C for 1 h, proteins of the pellets were resolved on SDS-PAGE under non-reducing conditions and immunoblotted with either anti-OxyR2 or anti-OxyR1 antibody (Bang *et al*., 2012).

*Site-directed mutagenesis of oxyR*2 *and purification of the mutant OxyR2 proteins*

Each of the seven cysteine residues in OxyR2 (C29, C49, C91, C104, C114, C206 and C215) was replaced with serine by using a QuikChange® Site-Directed Mutagenesis Kit (Agilent Technologies, Loveland, CO) (Bang *et al*., 2012). The complementary mutagenic primers listed in Table S1 were used in conjunction with the plasmid pDY1025 (*oxyR*2 on pJH0311 as a template DNA) to create pKSY017 (for OxyR2-C29S), pKSY018 (for OxyR2-C49S), pKSY019 (for OxyR2-C91S), pKSY020 (for OxyR2-C104S), pKSY021 (for OxyR2-C114S), pDY1104 (for OxyR2-C206S) and pDY1105 (for OxyR2-C215S) (Table 2).

Similar experimental conditions were used to replace the five cysteines in OxyR2 except for C206 and C215 with alanines. The complementary mutagenic primers listed in Table S1 were used in conjunction with the plasmid pDY1001 [*oxyR*2 on pET-28a (+) as a template DNA] to create pDY1014 (for $OxyR2_{5CA}$) (Table 2). The serine substitution of C206 or C215 was introduced into pDY1014 using the complementary mutagenic primers (Table S1) through the same procedures as described above, resulting in pDY1015 (for $OxyR2_{5CA}$-C206S) and pDY1016 (for $OxyR2_{5CA}$-C215S). The ORFs encoding $OxyR2_{5CA}$ from pDY1014 and $OxyR2_{5CA}$-C206S from pDY1015 were amplified by PCR using a pair of primers OXYR2C-F and -R (Table S1) and subcloned into pJH0311 to create pDY1026 and pDY1027 respectively (Table 2). All the mutations were confirmed by DNA sequencing. The mutant proteins were expressed, purified as described above, dialysed against storage buffer [20 mM Tris-HCl, pH 8.0, 250 mM NaCl, 1 mM dithiothreitol (DTT), and 50% (v/v) glycerol], and kept frozen at –80°C until use.

MALDI-TOF-MS analysis

To reduce OxyR2, 3 μM of His_6-tagged wild-type OxyR2 in a reaction buffer [20 mM Tris, pH 7.4, 0.3 M KCl, 5 mM $MgCl_2$, 0.5 mM EDTA, and 10% (v/v) glycerol] was treated with 100 mM DTT for 1 h, and then DTT was removed by gel filtration chromatography as described elsewhere (Lee *et al*., 2004; Bang *et al*., 2012). To oxidize OxyR2, the reduced OxyR2 was reacted with 30 μM H_2O_2 for 5 min after DTT removal. Subsequently, reduced cysteine residues of each reduced and oxidized OxyR2 were alkylated with 25 mM iodoacetamide for 1.5 h in dark under anaerobic condition. The reduced and oxidized OxyR2 proteins were resolved on non-reducing SDS-PAGE, and digested with trypsin (Sigma) as described previously (Bang *et al*., 2012). Peptides were extracted from the gel pieces with 0.1% trifluoroacetic acid in 50% acetonitrile, and MALDI-TOF-MS analyses were carried out on a Voyager-DE™ STR Biospectrometry Workstation (Applied Biosystems Inc., Foster City, CA). The masses of the cleavage peptides were determined using the PeptideMass software from the ExPASy proteomics server (http://us.expasy.org/tools/peptide-mass.html).

Electrophoretic mobility shift assay and DNase I protection assay

The 260 bp upstream region of *prx*2 promoter, extending from –246 to +14, was amplified by a PCR using [γ-^{32}P]-ATP-labelled PRX2P02-R and unlabelled PRX2P02-F as primers (Table S1). The labelled 260 bp DNA (5 nM) probe was incubated with various concentrations of purified $OxyR2_{5CA}$, $OxyR2_{5CA}$-C206S, or $OxyR2_{5CA}$-C215S for 30 min at 30°C in a 20 μl reaction mixture containing 1× binding buffer [25 mM Tris-Cl (pH 8.0), 25 mM KCl, 6 mM $MgCl_2$ 0.5 mM EDTA, 10% (v/v) glycerol, 0.05% (v/v) Tween20, 50 μg ml^{-1} BSA and 200 ng of poly (dI-dC) (Sigma)]. Electrophoretic analysis of the DNA-protein complexes has been described elsewhere (Lim and Choi, 2014).

The same labelled 260 bp DNA probe was used for the DNase I protection assays. The DNA-protein binding reactions with purified $OxyR2_{5CA}$, $OxyR2_{5CA}$-C206S, or $OxyR2_{5CA}$-C215S were performed as described above and DNase I digestion of the DNA-protein complexes followed the procedures previously described (Kim *et al*., 2011). After ethanol precipitation, the digested DNA products were resolved on a sequencing gel alongside sequencing ladders of pKSY036 generated using PRX2P02-R as a primer. The plasmid pKSY036 was constructed by cloning the same 260 bp upstream region of *prx*2 into pGEM-T Easy (Promega). The gels were visualized as described above for the transcript analysis.

Cytotoxicity and growth rate during infection

Cytotoxicity was evaluated by measuring cytoplasmic lactate dehydrogenase (LDH) activity that is released from the INT-407 human intestinal epithelial cells (ATCC CCL-6) by damage of plasma membranes. The INT-407 cells were grown in minimum essential medium containing 1% (v/v) fetal bovine serum (MEMF) (Gibco-BRL, Gaithersburg, MD) in 96-well culture dishes (Nunc, Roskilde, Denmark) as described previously (Lim and Choi, 2014). Each well with 2×10^4 INT-407 cells was infected with the *V. vulnificus* strains at a various moi for 1.5 h. The LDH activity released into the supernatant was determined using a cytotoxicity detection kit (Roche, Mannheim, Germany).

Growth rates of the bacterial strains during the infection were monitored (Oh *et al*., 2009). The INT-407 cells were infected using the wild type and *oxyR*2 mutant at an moi of 20. Samples of the supernatant of the INT-407 cells were removed at regular intervals and bacterial cells in the supernatant were determined by counting cfu on LBS agar plates.

Data analyses

All data representing the median values of results from at least three independent experiments were presented. Averages and standard errors of the mean (SEM) were also calculated from at least three independent experiments. The statistical significance of the difference among the *V. vulnificus* strains was evaluated using Student's *t*-tests with SAS program (SAS software; SAS Institute Inc., Cary, NC). Significance was accepted at a *P*-value of < 0.005.

Acknowledgements

This work was supported by Mid-career Researcher Program Grants 2012R1A2A1A03009679 through National Research Foundation funded by Ministry of Science, ICT, and Future Planning; and the R&D Convergence Center Support Program of the Ministry of Agriculture, Food and Rural Affairs, Republic of Korea (to S.H.C.).

References

Åslund, F., Beckwith, M., Zheng, J., and Storz, G. (1999) Regulation of the OxyR transcription factor by hydrogen peroxide and the cellular thiol – disulfide status. *Proc Natl Acad Sci USA* **96:** 6161–61665.

Baek, W.K., Lee, H.S., Oh, M.H., Koh, M.J., Kim, K.S., and Choi, S.H. (2009) Identification of the *Vibrio vulnificus ahpC*l gene and its influence on survival under oxidative stress and virulence. *J Microbiol* **47:** 624–632.

Bang, Y.J., Oh, M.H., and Choi, S.H. (2012) Distinct characteristics of two 2-Cys peroxiredoxins of *Vibrio vulnificus* suggesting differential roles in detoxifying oxidative stress. *J Biol Chem* **287:** 42516–42524.

Bsat, N., Chen, L., and Helmann, J.D. (1996) Mutation of the *Bacillus subtilis* alkyl hydroperoxide reductase (*ahpCF*) operon reveals compensatory interactions among hydrogen peroxide stress genes. *J Bacteriol* **178:** 6579–6586.

Choi, H.J., Kim, S.J., Mukhopadhyay, P., Cho, S., Woo, J.R., Storz, G., and Ryu, S.E. (2001) Structural basis of the redox switch in the OxyR transcription factor. *Cell* **105:** 103–113.

Christman, M.F., Morgan, R.W., Jacobson, F.S., and Ames, B.N. (1985) Positive control of a regulon for defenses against oxidative stress and some heat-shock proteins in *Salmonella typhimurium*. *Cell* **41:** 753–762.

Chung, K.J., Cho, E.J., Kim, M.K., Kim, Y.R., Kim, S.H., Yang, H.Y., *et al*. (2010) RtxA1-induced expression of the small GTPase Rac2 plays a key role in the pathogenicity of *Vibrio vulnificus*. *J Infect Dis* **201:** 97–105.

Dubbs, J.M., and Mongkolsuk, S. (2012) Peroxide-sensing transcriptional regulators in bacteria. *J Bacteriol* **194:** 5495–5503.

Goo, S.Y., Lee, H.-J., Kim, W.H., Han, K.-L., Park, D.-K., Lee, H.-J., *et al*. (2006) Identification of OmpU of *Vibrio vulnificus* as a fibronectin-binding protein and its role in bacterial pathogenesis. *Infect Immun* **74:** 5586–5594.

Hall, A., Karplus, P.A., and Poole, L.B. (2009) Typical 2-Cys peroxiredoxins–structures, mechanisms and functions. *FEBS J* **276:** 2469–2477.

Jacobson, F.S., Morgan, R.W., Christman, M.F., and Ames, B.N. (1989) An alkyl hydroperoxide reductase from *Salmonella typhimurium* involved in the defense of DNA against oxidative damage. *J Biol Chem* **264:** 1488–1496.

Kelley, L.A., and Sternberg, M.J. (2009) Protein structure prediction on the web: a case study using the Phyre server. *Nat Protoc* **4:** 363–371.

Kim, B.S., Hwang, J., Kim, M.H., and Choi, S.H. (2011) Cooperative regulation of the *Vibrio vulnificus nan* gene cluster by NanR protein, cAMP receptor protein, and N-acetylmannosamine 6-phosphate. *J Biol Chem* **286:** 40889–40899.

Kim, S.O., Merchant, K., Nudelman, R., Beyer, W.F., Jr, Keng, T., DeAngelo, J., *et al*. (2002) OxyR: a molecular code for redox-related signaling. *Cell* **109:** 383–396.

Kong, I.S., Bates, T.C., Hulsmann, A., Hassan, H., Smith, B.E., and Oliver, J.D. (2004) Role of catalase and *oxyR* in the viable but nonculturable state of *Vibrio vulnificus*. *FEMS Microbiol Ecol* **50:** 133–142.

Kullik, I., Stevens, J., Toledano, M.B., and Storz, G. (1995a) Mutational analysis of the redox-sensitive transcriptional regulator OxyR: regions important for DNA binding and multimerization. *J Bacteriol* **177:** 1285–1291.

Kullik, I., Toledano, M.B., Tartaglia, L.A., and Storz, G. (1995b) Mutational analysis of the redox-sensitive transcriptional regulator OxyR: regions important for oxidation and transcriptional activation. *J Bacteriol* **177:** 1275–1284.

Kunisaki, H., and Tanji, Y. (2010) Intercrossing of phage genomes in a phage cocktail and stable coexistence with *Escherichia coli* O157:H7 in anaerobic continuous culture. *Appl Microbiol Biotechnol* **85:** 1533–1540.

Lee, C., Lee, S.M., Mukhopadhyay, P., Kim, S.J., Lee, S.C., Ahn, W.S., *et al*. (2004) Redox regulation of OxyR requires specific disulfide bond formation involving a rapid kinetic reaction path. *Nat Struct Mol Biol* **11:** 1179–1185.

Lim, J.G., and Choi, S.H. (2014) IscR is a global regulator essential for the pathogenesis of *Vibrio vulnificus* and induced by host cells. *Infect Immun* **82:** 569–578.

Miller, R.A., and Britigan, B.E. (1997) Role of oxidants in microbial pathophysiology. *Clin Microbiol Rev* **10:** 1–18.

Miller, V.L., and Mekalanos, J.J. (1988) A novel suicide vector and its use in construction of insertion mutations: osmoregulation of outer membrane proteins and virulence determinants in *Vibrio cholerae* requires *toxR*. *J Bacteriol* **170:** 2575–2583.

Milton, D.L., O'Toole, R., Horstedt, P., and Wolf-Watz, H. (1996) Flagellin A is essential for the virulence of *Vibrio anguillarum*. *J Bacteriol* **178:** 1310–1319.

Netto, L.E., de Oliveira, M.A., Monteiro, G., Demasi, A.P., Cussiol, J.R., Discola, K.F., *et al*. (2007) Reactive cysteine in proteins: protein folding, antioxidant defense, redox signaling and more. *Comp Biochem Physiol C Toxicol Pharmacol* **146:** 180–193.

Oh, M.H., Jeong, H.G., and Choi, S.H. (2008) Proteomic identification and characterization of *Vibrio vulnificus* proteins induced upon exposure to INT-407 intestinal epithelial cells. *J Microbiol Biotechnol* **18:** 968.

Oh, M.H., Lee, S.M., Lee, D.H., and Choi, S.H. (2009) Regulation of the *Vibrio vulnificus hupA* gene by temperature alteration and cyclic AMP receptor protein and evaluation of its role in virulence. *Infect Immun* **77:** 1208–1215.

Oka, A., Sugisaki, H., and Takanami, M. (1981) Nucleotide sequence of the kanamycin resistance transposon Tn903. *J Mol Biol* **147:** 217–226.

Sambrook, J., and Russell, D. (2001) *Molecular Cloning: A Laboratory Manual*, 3rd edn. New York: Cold Spring Horbor laboratory Press.

Seaver, L.C., and Imlay, J.A. (2001) Alkyl hydroperoxide reductase is the primary scavenger of endogenous hydrogen peroxide in *Escherichia coli*. *J Bacteriol* **183:** 7173–7181.

Seth, D., Hausladen, A., Wang, Y.J., and Stamler, J.S. (2012) Endogenous protein S-nitrosylation in *E. coli*: regulation by OxyR. *Science* **336:** 470–473.

Storz, G., and Zheng, M. (2000) Oxidative stress. In *Bacterial Stress Responses*. Storz, G., and Hengge-Aronis, R. (eds). Washington, DC: ASM Press, pp. 47–59.

Storz, G., Jacobson, F., Tartaglia, L., Morgan, R., Silveira, L., and Ames, B. (1989) An alkyl hydroperoxide reductase induced by oxidative stress in *Salmonella typhimurium* and *Escherichia coli*: genetic characterization and cloning of *ahp*. *J Bacteriol* **171:** 2049–2055.

Storz, G., Tartaglia, L.A., and Ames, B.N. (1990) Transcriptional regulator of oxidative stress-inducible genes: direct activation by oxidation. *Science* **248:** 189–194.

Tao, K., Makino, K., Yonei, S., Nakata, A., and Shinagawa, H. (1991) Purification and characterization of the *Escherichia coli* OxyR protein, the positive regulator for a hydrogen peroxide-inducible regulon. *J Biochem* **109:** 262–266.

Tao, K., Fujita, N., and Ishihama, A. (1993) Involvement of the RNA polymerase α subunit C-terminal region in cooperative interaction and transcriptional activation with OxyR protein. *Mol Microbiol* **7:** 859–864.

Toledano, M.B., Kullik, I., Trinh, F., Balrd, P.T., Schnelder, T.D., and Storz, G. (1994) Redox-dependent shift of OxyR-DNA contacts along an extended DNA-binding site: a mechanism for differential promoter selection. *Cell* **78:** 897–909.

Wang, X., Mukhopadhyay, P., Wood, M.J., Outten, F.W., Opdyke, J.A., and Storz, G. (2006) Mutational analysis to define an activating region on the redox-sensitive transcriptional regulator OxyR. *J Bacteriol* **188:** 8335–8342.

Zaim, J., and Kierzek, A.M. (2003) The structure of full-length LysR-type transcriptional regulators. Modeling of the full-length OxyR transcription factor dimer. *Nucleic Acids Res* **31:** 1444–1454.

Zheng, M., Aslund, F., and Storz, G. (1998) Activation of the OxyR transcription factor by reversible disulfide bond formation. *Science* **279:** 1718–1722.

Zheng, M., Wang, X., Templeton, L.J., Smulski, D.R., LaRossa, R.A., and Storz, G. (2001) DNA microarray-mediated transcriptional profiling of the *Escherichia coli* response to hydrogen peroxide. *J Bacteriol* **183:** 4562–4570.

Supporting information

Additional supporting information may be found in the online version of this article at the publisher's web-site.